Hybrid Material for Screen Protection of Foldable Devices

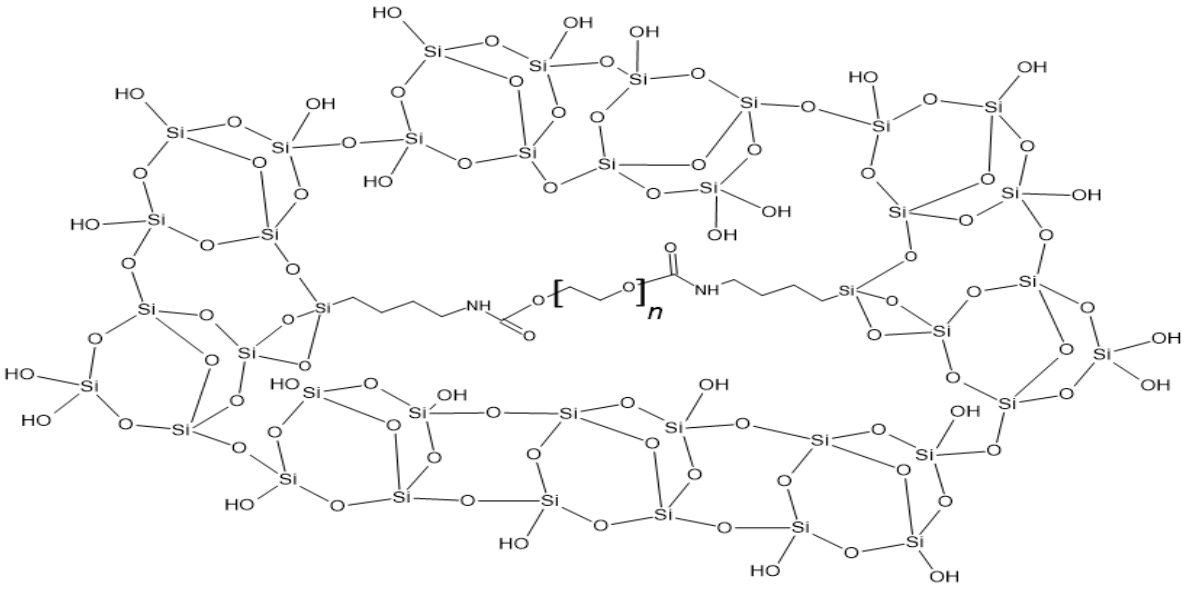

Group Bio-24-kbt-7-d1

December 20, 2024

Chemical Engineering Bachelor Thesis

Seventh Semester

Aalborg University

AALBORG UNIVERSITY

STUDENT REPORT

Faculty of Engineering and Science
Department of Chemistry and Bioscience
Chemical Engineering
Fredrik Bajers Vej 7H
9220 Aalborg East
https://www.en.bio.aau.dk/

Title:

Hybrid Material for Screen Protection of Foldable Devices

Theme:

Chemical Engineering Bachelor Thesis

Project Period:

3. September 2024 - 20. December 2024

Field of study:

Chemical Engineering

Project Group:

Bio-24-kbt-7-d1

Participants:

Hans Nikolai Sørensen
Mathias Flugt Sørensen
Nikolai Haugaard Jensen
Wojciech Luterek

Supervisors:

Anders Mose Schade
Donghong Yu

Number of Pages: 26
Appendix: (11)
Date of Completion: December 20, 2024

Abstract:

Smartphones are widely used globally, and there is a growing interest in foldable devices like the Samsung Galaxy Flip 5. These foldable screens are fragile, so new protection solutions are needed, as the existing are inadequate. This project explores the possibility of screen protection for foldable devices, using a sol-gel method to create a hybrid material with tetraethyl orthosilicate (TEOS), polyethylene glycol (PEG), and 3-(triethoxysilyl)-propyl isocyanate (TPI). The precursors are mixed in a two step reaction then aged, and then analyzed for their properties. The best result is obtained with TPI molar ratio 2.0 to PEG, which had been catalyzed using dibutyltin dilaurate (DBTL), which results in type II bonding that improves the materials network strength.
The materials show good transparency, and adjusting the TPI ratio changes the hardness and flexibility of the hybrid materials. Using DBTL as a catalyst improves the hybrid materials thermal stability and water stability. This indicates better network connectivity between the polymer and coupling agent, through covalent bonds. It is the coupling agent's inorganic sites that connect to the silica network through condensation reactions, which is also visible in the FTIR analysis.

Preface

This bachelor thesis report is written by B.Eng. students in chemical engineering. The report is a product of 7^{th} semester project from PanzerGlass®, where the main study is to produce and analyze flexible transparent hybrid material made with the sol-gel technique. The language of the report is in American English and punctuation is done according to the Oxford comma.

Sources are cited using the IEEE citation style. Illustrations and tables are numbered by sections, sources for all illustrations are available in the figure text. The abbreviations used in this report are provided on page IV. Knowledge obtained in this report is sourced from peer reviewed research articles, and the experience gained from synthesis and trial and error approach with the sol-gel glass optimization. Artificial intelligence has been partially used in this report to aid with grammar correction.

The nomenclature used for materials in this report is as follows:

Agent(ratio)-Polymer-Catalyst-TEOS(time)-State-No.
EX: TPI1.0-PEG200-N-TEOS30-S-a
Bridging agent, ratio of agent - Polymer - [N]oncatalyst/[C]atalyst
- Time mixed with teos in min - [L]iquid/[S]olid-No. if identical.

The bachelor thesis group would like to thank Anders M. Schade with the project supervision and assistance in the laboratory. The group would also thank the institute of Chemistry and Bioscience for providing the laboratory facilities and equipment necessary for this project.

Hans Nikolai Sørensen
Studienr: 20204674
hsaren20@student.aau.dk

Mathias Flugt Sørensen
Studienr: 20214137
msorec21@student.aau.dk

Nikolai Haugaard Jensen
Studienr: 20214967
nikolj21@student.aau.dk

Wojciech Luterek
Studienr: 20213453
wluter21@student.aau.dk

List of abbreviations

ATR Attenuated Total Reflectance. V, 7, 11, 13, 14

DBTL Dibutyltin Dilaurate. 11, 18, 19, 20, 25, xi

FTIR Fourier Transform Infrared Spectroscopy. V, 3, 7, 8, 11, 13, 14, 15, 16, 17, 18, 19, 20, 23, 25, viii

GPTMS (3-glycidyloxypropyl)trimethoxysilane. 2, 9, 10, 13, 14

PEG Polyethylene Glycol. V, 2, 8, 9, 10, 11, 14, 15, 16, 17, 18, 19, 20, 22, 23, 24, 25, 26, iv

TEOS Tetraethyl Orthosilicate. V, 2, 4, 6, 8, 9, 10, 11, 13, 16, 18, 25, 26

TGA Thermogravimetric Analysis. V, 3, 12, 24, 25

THF Tetrahydrofuran. 10, 11, 17, 24

TPI 3-(triethoxysilyl)-propyl isocyanate. V, 2, 8, 10, 11, 14, 15, 16, 17, 18, 19, 20, 22, 23, 24, 25, 26, ii, iii, vi, vii

TPU Thermoplastic Polyurethane. 1, 3, 26

Contents

1 Introduction

Approximately 43% of Americans will get a cracked phone screen replaced either through warranty, insurance, or own expense[1]. There are products on the market that can prevent damage to the device such as device covers, and screen protectors, made of tempered thin glass or plastic film[2].

In 2018, Royole FlexPai was revealed as the world's first smartphone with a foldable screen. The same year, Samsung revealed its vision to create a foldable phone [3]. Since then several new entries in this category have been put on the market. The first foldable phones had an Organic Light-Emitting Diode (OLED) screen with a polymer protection layer, newer phones have an ultra-thin and flexible oxide glass screen. This glass screen is very fragile and easily damaged by scratching and direct impact [4][5].

For the consumer, the cost of replacing a foldable screen ranges from 300 USD to 1010 USD, depending on the phone model [6][7]. Repairing the screen is costly, often nearing the phone's value. Therefore, screen protection for ultra-thin glass screens which is cheaper than replacing the screen, is preferred from a consumer standpoint. The current screen protection for foldable phones are Thermoplastic Polyurethane (TPU) films. They are used due to their good elasticity and flexibility. However, TPU lacks sufficient scratch and drop resistance. More robust screen protectors, as those made of tempered glass have a higher drop resistance, protecting the phone when being dropped on hard surfaces, by the tempered glass shattering instead of the phone. Tempered glass protection are thicker and more rigid than TPU films, making them unsuitable for foldable devices. Thereby, despite low drop resistance, TPU films remain the best screen protector option for foldable devices. [2][8].

Consequently, there is an ongoing interest in developing new screen protectors that combine flexibility and strength to endure frequent folding and unfolding, while offering improved drop and scratch resistance. Researchers are exploring organic-inorganic hybrids, incorporating the strength of inorganic silica (SiO_2) with the flexibility of organic polymers through the sol-gel method [9] [10]. This process involves mixing the constituents in a liquid phase and gradually removing the solvent through evaporation [11].

The hybrid sol-gel approach leverages the nanoscale mixing of organic and inorganic materials at a molecular level, which includes type I and II materials. Type I hybrids applies weaker intermolecular forces to stabilize the system resulting in physically embedded polymers in an inorganic matrix. In type II materials, organic and inorganic parts are bonded and the system is stabilized by strong intramolecular forces, like covalent bonds [12]. An example of a hybrid sol-gel material is tetraethyl orthosilicate (TEOS), which is hydrolyzed by acidic catalysis and mixed with a polymer. The hydrolysis produces hydroxyl groups that can then react further in a condensation reaction. During evaporation of the solvent, the reaction will form a amorphous structure with the polymer in the silica matrix. Depending on the polymer, it can bind to the matrix or lie in between, thus creating a material with unique properties [13].

In hybrid sol-gel materials, a polymer as Polyethylene Glycol (PEG) can introduce elastomeric properties to an inorganic network. By varying average molecular weight, 200, 600, 1000 Da, the properties of the hybrid glass can be fine tuned to suit desirable traits like flexibility while maintaining structural integrity[14]. To have a tougher and stronger material for example a screen protector, type II to bonds are preferred. The addition of PEG to the sol-gel does not guarantee type II bonds. To increase the probability of type II bonds, a coupling agent can by used to create chemical bonds between the inorganic silica network and organic polymer. Typically, silane-based agents like (3-glycidyloxypropyl)trimethoxysilane (GPTMS) or 3-(triethoxysilyl)-propyl isocyanate (TPI) are used with a TEOS precursor.

Thesis Statement 2

As more foldable smartphones enter the market, the need for durable screen protection increases, due to the current TPU screen protectors being inadequate. A promising approach for creating a flexible material is the hybrid sol-gel method which incorporates a polymer into a silica network. Coupling agents can be used to facilitate the covalent bonding between the organic and inorganic molecules which otherwise can be a challenge. Therefore, the aim of this report is:

With varying molar ratios of coupling agent, investigate the improvements of the covalent bonding in the TEOS/PEG system, to find the most stable hybrid material.

To determine properties of the hybrid material, Fourier Transform Infrared Spectroscopy (FTIR), Thermogravimetric Analysis (TGA), and qualitative assessment will be performed.

Theory 3

3.1 Sol-gel Method

Sol-gel method is a low-temperature process. The benefits of the low-temperature process are that the energy required for creating a glass material is much lower than the traditional melting and quenching method, thereby making a possible cheaper and more environmental friendly product. The sol-gel method is possible as liquid silica precursors like TEOS, also known as an metal alkoxide, is hydrolyzed. The reaction time of the hydrolysis can be adjusted, by adjusting either the pH or temperature. Water is used to hydrolyze the metal alkoxides in acidic or alkaline conditions[13].

The hydrolysis of a Si-based metal alkoxide, follows the equation below [13]:

$$Si(OR)_n + jH_2O \longrightarrow Si(OH)_jOR_{n-j} + jROH[13] \tag{3.1}$$

TEOS is used as an example in Equation 3.1,; $n = 4$ as Si has tetrahedral geometry, therefore Si forms bonds with 4 alkoxy groups (-OR). $R = C_2H_5$, alkyl groups can vary depending on the silicon-based alkoxide; in this example, TEOS is used, which has ethyl groups. $j = 1, ..., n$, shows how many of the original n alkoxy groups have been replaced by hydroxyl groups (-OH), which varies depending on how many -OR groups have been hydrolyzed. When the first condensation reaction occurs, it can appear as follows in Equation 3.2:

$$Si(OH)_i(OR)_{n-i}+Si(OH)_k(OR)_{n-k} \longrightarrow Si{-}O{-}Si(OH)_{i+k-1}(OR)_{2n-i-k-1}+ROH[13] \tag{3.2}$$

In Equation 3.2, i and k denote the number of hydroxyl groups (-OH) present on each of the condensing SiO_2 atoms. The hydroxyl groups on these Si atoms can condense to form siloxane bonds ($Si{-}O{-}Si$), releasing ethanol as a by-product in an equilibrium, which can be shifted towards the siloxane bonds by evaporating the ethanol. The silica network is expanded through condensation with other hydrolyzed silica, forming colloidal silica particles; however, further condensation leads to long polymer chains as in Equation 3.3:

$$(Si{-}O{-})_mSi(OH)_j(OR)_{n(2m+1)-2m-j}[13] \tag{3.3}$$

Equation 3.3 describes the extended polymerized silica network with m siloxane bonds, j counting -OH groups still attached to silicon, and $n(2m+1) - 2m - j$ representing -OR groups remaining.

3.1.1 Hybrid Sol-gel Material

As presented in the Section 3.1, a usual sol-gel synthesis is initiated by a catalyzed hydrolysis and condensation of a silica metal alkoxide precursor. Doing sol-gel method with only a silica metal alkoxide precursor will consequently result in a highly porous structure. These highly porous materials have poor mechanical properties, including brittleness and low strength, regardless of processing method. This issue is solved by incorporating an organic polymer paired with the silica precursor, based on chemical compatibilities [15][16][17].

Incorporating an organic polymer paired with the silica precursor, can be done by the hybrid sol-gel method. A hybrid organic-inorganic sol-gel material includes two moieties mixed on a molecular scale. As stated in Chapter 1, hybrid sol-gel material is divided into type I and II. Type I hybrid materials are characterized by weak chemical interactions between the two phases, such as intermolecular forces. Type II hybrid materials are characterized by strong chemical interactions between their organic and inorganic components. These materials are primarily held together by stronger intramolecular bonds, which provide enhanced stability to the system.[12]

3.1.2 Crosslinking in the Sol-gel Process

Crosslinking is known in the rubber industry for producing a stronger material by limiting the structural mobility of the polymer by linking two sites together using a crosslinker. In hybrid sol-gel based materials, the polymers creates crosslinks between the silica particles, through the attached coupling agent [18].

It is important to consider the ratio of the coupling agent while taking into account how many coupling sites there are, and where these sites are located in the material. By tweaking the ratio of the coupling agent, an optimal network can be created with the desired properties [18].

During crosslinking processes, three possible scenarios can occur, see Figure 3.1 for a visual representation of these scenarios:
Null-binding occurs when there is an unreacted polymer remaining in the sample. The substituents will not be bound by covalent bonds, but can still be in the final material, because of intermolecular forces.
Capping occurs when a polymer reacts only at one end, resulting in a covalent bond at that end of the material. The other end may have intermolecular forces, which do not contribute to the desired structure. Crosslinking is where both polymer ends are bonded to a coupling agent incorporated in the silica network[19].

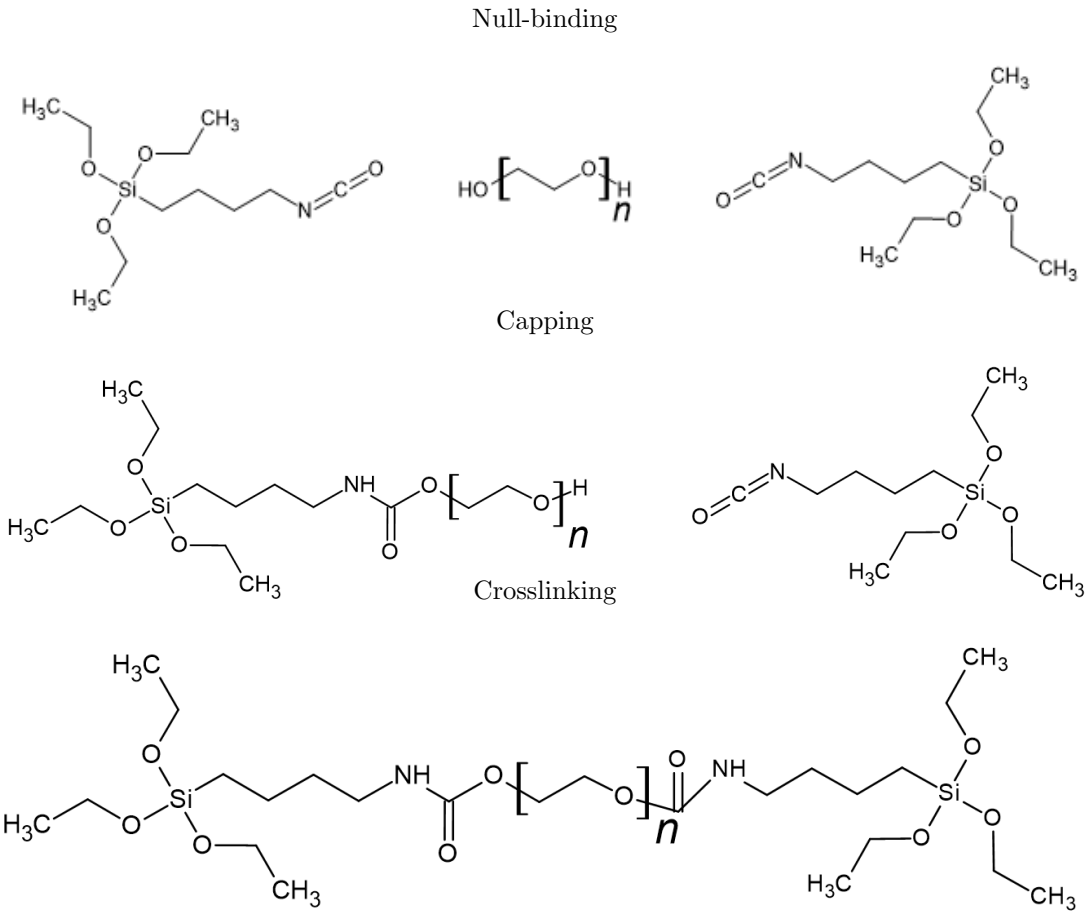

Figure 3.1. Visualization of null-binding, capping, and crosslinking, the inorganic end of the coupling agent needs to bind to TEOS.

Both null-binding and capping increases when the ratio of polymer to coupling agent is above the ideal ratio for the mixture. The theoretical molar ratio for achieving the most crosslinking is 1:2 polymer:coupling agent, as this means everything will have a site to react with. But as null-binding and capping always can occur, this ideal ratio is often varying depending on the scenarios and substituent used [19].

3.2 Fourier Transform Infrared Spectroscopy (FTIR)

Infrared spectroscopy is a method for analyzing how infrared electromagnetic radiation affects different types of chemical bonds. FTIR is often performed in the wavelengths between $4000\,\mathrm{cm}^{-1}$ and $400\,\mathrm{cm}^{-1}$, called the mid-infrared region. The method measures the change in dipole moment, caused by the absorbance of the radiation, trough rotational and vibrational transitions [20].

Absorption of the radiation that does not cause a change in the dipole moment, cannot be measured with infrared spectroscopy. The measurement is Fourier transformed, which is a mathematical method for dividing a varying signal into the simplest frequencies of which it is made up [20].

An example of a molecule interacting with the infrared beam can be water. Water can absorb the radiation and vibrate by a symmetric bending, symmetric stretch and asymmetric stretch. Any and all of these vibration types can happen when exposed to the beam. So in general, when peaks are located in a spectrum between $3000\,\mathrm{cm}^{-1}$ to $3700\,\mathrm{cm}^{-1}$, it indicates that water is in the sample. In larger molecules, the vibrations may change the dipole moment in some parts of the molecule but not in others so each peak can in general be assigned to a specific functional group [20].

Attenuated Total Reflectance (ATR) can analyze all types of samples except gases. This mode is an excellent method for analyzing a wide range of samples, because it has a quick and easy sample preparation. As seen in Figure 3.2 the ATR generates a infrared spectra by pressing the sample down on an ATR crystal. Then the infrared beam travels through the ATR crystal to the sample and afterwards back through the crystal to the detector. The interaction between the beam and the crystal will result in internal reflections that generates a wave with the ability to penetrate a few microns into the sample. Then the wave is reflected back with either an alteration or a reduction in the strength of the signal [20][21].

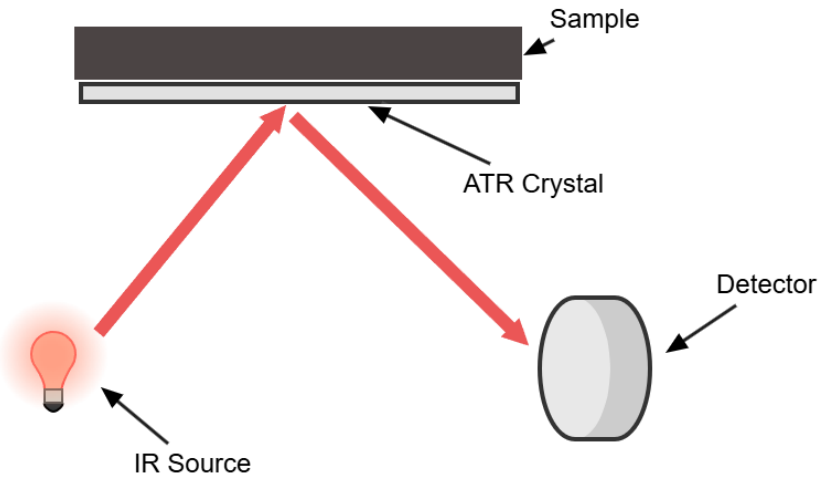

Figure 3.2. Illustration of how the ATR crystal reflects the IR beam to the detector. Illustrated using chemix.org.[22]

3.2.1 Expected peaks from the FTIR spectra

The synthesis of the hybrid glass will lead to specific molecular bonds forming. The primary bonds will be inorganic Si−O bonds, which originate from the hydrolysis and condensation of TEOS and TPI. Secondly, the bonds forming from the reaction between TPI and PEG to generate a carbamate group [23]. These bonds are IR compatible and will show in the spectra. Because of the chemical environment, precise predictions on the exact wave number that corresponds to a specific functional group can not be done. But an estimate can be found in literature on what wave interval each functional group has, see Figure 3.3 and Appendix Table A.1 [24]. Furthermore, similar experiments on hybrid glass can support the estimate [9][25][26].

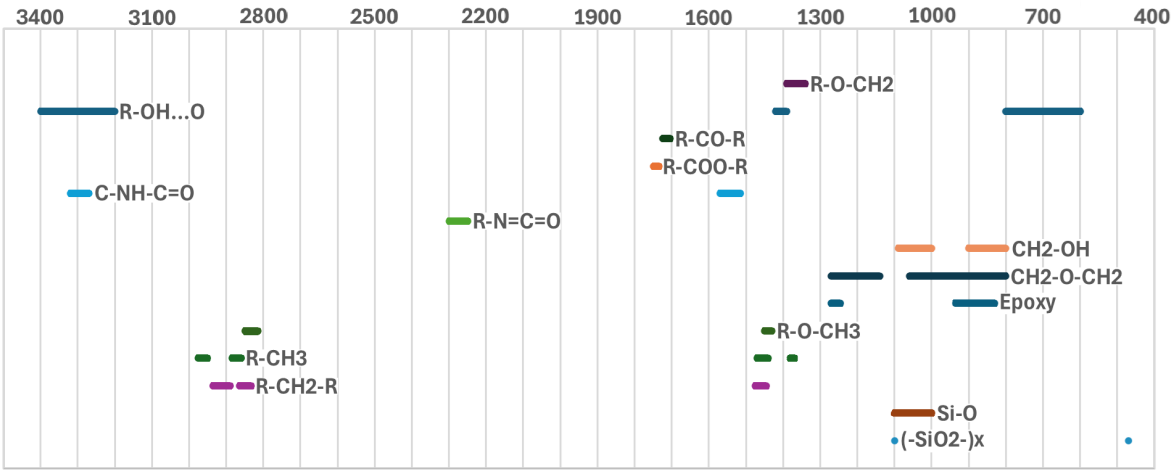

Figure 3.3. Showing the estimate for wave number interval that each functional group has, which is found in literature [24].

Materials & methods 4

4.1 Sol-gel Hybrid Material Synthesis

The preparation of the sol-gel in this report can be divided into two parts; TEOS hydrolysis and mixing the polymer/coupling agent.

4.1.1 TEOS Hydrolyzation

Table 4.1. List of chemicals used in the hydrolysis reaction, and their respective molar ratios.

Chemical	Brand	Comment	Molar Ratio
Tetraethyl Orthosilicate	Sigma-Aldrich	98%	1
H_2O		Demineralized	4
HCl	VWR Chemicals	35 w/w%	0.01

A recurring part of the sol-gel synthesis is the hydrolysis of TEOS. Hydrolysis of TEOS is carried out by mixing TEOS with demineralized water and using HCl as a catalyst, using chemicals mentioned in Table 4.1. The solution is mixed for approximately 15 to 30 minutes until the solution goes from hazy to clear. The molar ratio of the chemicals used for the TEOS hydrolyzation reaction are mentioned in Table 4.1.

4.1.2 GPTMS Reaction

Table 4.2. List of chemicals used in the GPTMS reactions and their respective molar ratios.

Chemical	Brand	Comment	Molar Ratio
Ethanol (absolute)	VWR Chemicals	99.9%	1
Polyethylene Glycol (M_n200)	Sigma-Aldrich	Laboratory grade	1
(3-glycidyloxypropyl)trimethoxysilane	Sigma-Aldrich	98%	0.25

The synthesis using GPTMS is a one-pot reaction, using chemicals mentioned in Table 4.2 with the given molar ratios. Ethanol is added to the clear hydrolyzed TEOS from Section 4.1.1. Shortly after the addition of ethanol, PEG200 and GPTMS are added in quick succession. The sol is then stirred for an hour at room temperature. After one hour, the sol is poured in a closed container, and placed in an oven at 40 °C for aging to occur, and after sufficient aging the container is opened for evaporation of the solvent to occur. The container is weighed once a day to monitor the evaporation of solvent from the sample. When the weight is stable, the material is ready.

4.1.3 TPI Reaction

Table 4.3. List of chemicals used in the TPI reactions and their respective molar ratios, with n*, being the molar ratio range (0.1, 0.25, 0.5, 1.0, 2.0).

Chemical	Brand	Comment	Molar Ratio
Tetrahydrofuran	VWR Chemicals	HPLC grade	1
Polyethylene Glycol (M_n200)	Sigma-Aldrich	Laboratory grade	1
3-(triethoxysilyl)-propyl isocyanate	Sigma-Aldrich	95%	n*

The synthesis using TPI is a two-pot reaction, where the hydrolyzed TEOS from Section 4.1.1 is done separately from the reaction between TPI and PEG. The chemicals used are shown in Table 4.3.

The polymer PEG and coupling agent TPI is combined in a three-neck round-bottom flask. It is important to keep an atmosphere in the flask of inert gas as TPI reacts with oxygen and water in the air. TPIs reaction with water is also the reason for using THF as a solvent.
For the synthesis using TPI; PEG, THF and TPI is added to the container and mixed for 60 minutes. After the 60 minutes, the TEOS solution is added to the PEG/TPI mix and stirred for 30 minutes. The sol mixture is poured into a closed container and the aging and evaporation process are performed in the same way as the synthesis with GPTMS. The procedure is shown in Figure 4.1.

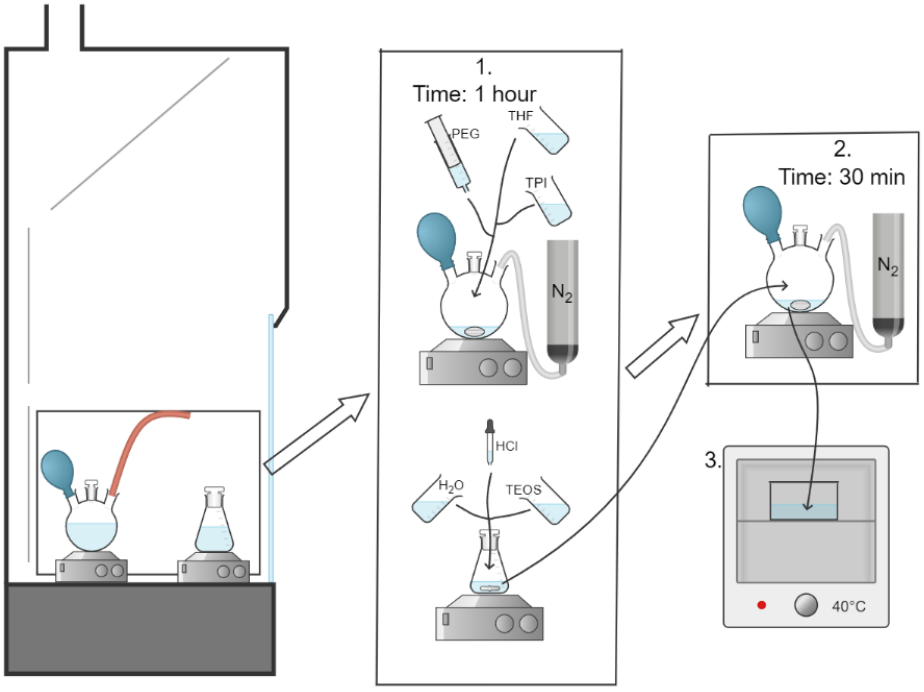

Figure 4.1. Setup for the TEOS - TPI reaction. Illustration is made using chemix.org.

4.1.3.1 Catalyzed Reaction

Table 4.4. List of chemicals used in the TPI reactions and their respective molar ratios, with n*, being the molar ratio range (0.25, 0.5, 1.0, 2.0, 3.0), and n** being varied respectively to n* by 10 w/w% of TPI.

Chemical	Brand	Comment	Molar Ratio
Tetrahydrofuran	VWR Chemicals	HPLC grade	1
Polyethylene Glycol (M_n200)	Sigma-Aldrich	Laboratory grade	1
3-(triethoxysilyl)-propyl isocyanate	Sigma-Aldrich	95%	n*
Dibutyltin Dilaurate	FLUKA	Laboratory grade	n**

The catalyzed reactions are performed similar to the non-catalyzed synthesis with the difference that the catalyst dibutyltin dilaurate DBTL is added to the TPI/PEG solution in a 10 w/w % to TPI. This is done, as the catalyst is used to catalyze the reaction of the hydroxyl group from PEG with the isocyanate group of the TPI[9]. For both catalyzed and non-catalyzed reaction the TPI ratio varies and the molar ratios used in the reactions are shown in Table 4.4.

All of the synthesized TEOS, PEG, and TPI hybrid materials and their information can be seen in Appendix F.

4.2 ATR-FTIR

When analyzing samples with ATR-FTIR , the procedure begins by cleaning the ATR (*Bruker TENSOR 2 FTIR, using Bruker Platinum ATR with diamond crystal*) surface to remove any residues from previous measurements. A background scan is then performed to establish a reference. Once complete, a sample piece large enough to cover the detector surface is placed on the ATR and pressed firmly to ensure good contact. When there is no significant change in the signal and peaks are visible, the measurement is performed with the following settings; *number of scans: 64, gas flow: 400 mL/min.* To compare samples normalization of the spectras is carried out, by dividing the intensity of the spectra with their largest intensity, meaning max value becomes 1.

4.3 Performance & Visual Assessment

This method is made to provide an overall score to the hybrid material produced, indicating the hybrid materials visual appearance, hardness, and flexibility . These assessments are purely qualitative from direct observations of the material. To be able to rate the materials, a scale is defined in each category ranging from 1 to 5, to later give an overall score which is a summary of the categories.

A score of 5 in transparency is given to a material that is clear. Color, bubbles, haziness, and crystallization lowers the score.
The firmness is evaluated by how soft the material felt when squeezed, the lower the score the more the material can be squeezed, a material with a score of 5 means that it can not be squeezed even when applying a large force.
The flexibility of the material is a rating of how the material flex when handling it with hands, a rating of 1 means that the material can not flex, and a 5 will be a material that can clearly flex more that 90°.
The toughness is evaluated by pressing a glass spatula vertically on the material an evaluating the force needed for it to brake, a score of 5 is a material that do not brake or requires a lot of force to break, a 1 is a material that are very brittle.
For surface a score of 5 is given to a material that have a smooth and dry surface, impurities, liquids, and stickiness lowers the score.

4.4 Water Resistance Test

A sample piece is weighed before being submerged in demineralized water for 24 hours on a mixing table. After the 24 hours time period, the samples are then taken out and dried off with paper towel, and put in a oven at 40°C for 60 minutes. After the excess water removal the samples are weighed and analyzed in the ATR-FTIR with the same settings as described in Section 4.2.

4.5 Thermogravimetric Analysis (TGA)

A sample piece is weighed before being put in aluminum crucible where TGA is done using the *NETZSCH STA 449 Jupiter*. Sample is heated up to 600°C with a step of 10K/min using He inert atmosphere with a flow of 20 mL/min.

Results & Discussion 5

5.1 Synthesis with GPTMS & Aging Time Experiment

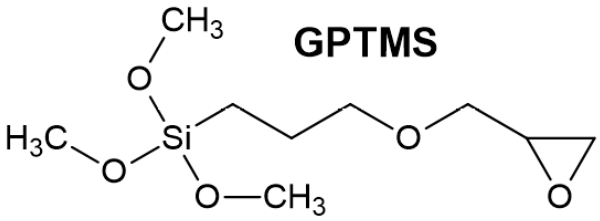

Figure 5.1. The structure of GPTMS, drawn using chem-sketch.

The epoxide group on GPTMS (Figure 5.1) should react with the hydroxyl sites on PEG, forming a bridge with both ends able to bind to the hydrolyzed TEOS particles. GPTMS is used because literature indicates the previously described interactions will occur [10][26]. Initial experiments showed that reactions did occur; however, the product had complications, such as reacting with water in the air and being a fragile material.

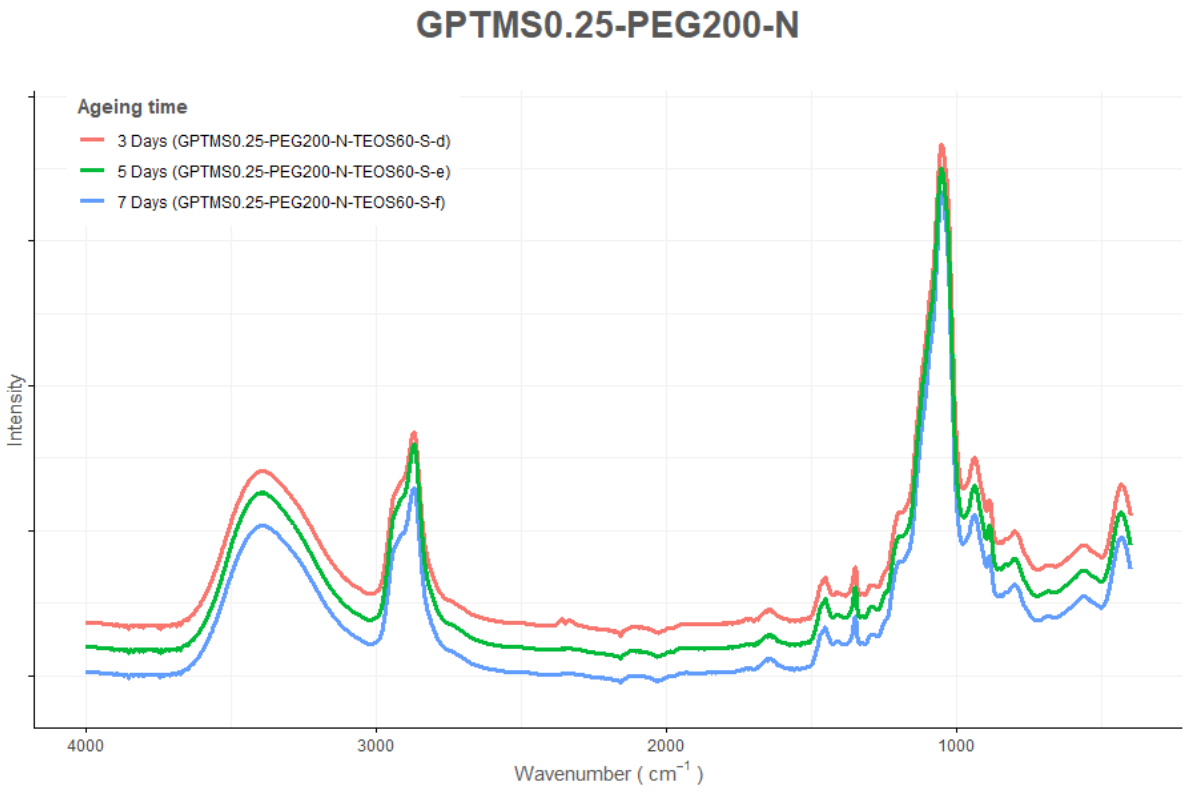

Figure 5.2. ATR-FTIR of tree different aging periods red 3 days, green 5 days, and blue 7 days. Each data set is normalized by dividing y values with the max y value, and up shifted by 0.05 in y-axis to make it more visible.

Further testing was conducted to validate the initial experiments, with experiments performed at fixed aging intervals. The results, as shown in Figure 5.2, display aging times of 3, 5, and 7 days. None of the samples exhibit additional peak changes on the FTIR compared to one another. The intensities of the samples are very similar, indicating that the difference in aging time did not influence the network of the material. The small differences observed may be due to signal error or background noise from the ATR.

Figure 5.3. Picture of the tree different aging periods, from left: 3 days, 5 days and 7 days.

Observations using GPTMS indicate that different aging intervals does not influence the overall structural integrity of the samples, which can be seen in Figure 5.3. This was evident to the naked eye after after opening the container lid to evaporate the solvent. Here the samples immediately experienced stress from the rapid solvent loss, shattering into smaller pieces within one day. This might be avoided by slowly evaporating the solvent through a more controlled method, however, this approach extend the aging time, which may not be favorable for industrial applications.

The silica, PEG200, and GPTMS network displayed overall poor flexibility, as even a slight bend caused the material to break. This led the project to explore another coupling agent with a more reactive site, potentially forming a stronger network capable of withstanding both the stress from solvent evaporation and breakage due to bending. The alternative coupling agent TPI was used for further material synthesis.

5.2 Comparison of Different Molar Ratios of TPI

The isocyanate group in TPI Figure 5.4, should bind to the hydroxyl-group in the end of the PEG chain, by breaking the double bond between carbon and nitrogen, binding the oxygen to carbon and hydrogen to the nitrogen [9].

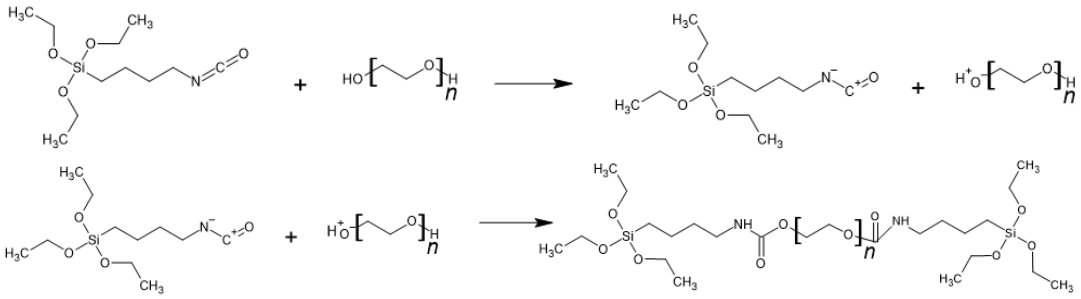

Figure 5.4. The structure of TPI and reation with PEG, drawn using chem-sketch.[9]

The aging time results from Section 5.1, was assumed to be the same in the future experiments, despite a different coupling agent, as it was thought to not influence it.

For at better understanding of the structural differences from the TPI:Polymer ratio and to see if the right reaction occured, FTIR data is used, see Figure 5.5 below. To better discuss the data, it will be sectioned into three regions; $3000cm^{-1}$ to $2750cm^{-1}$, $1700cm^{-1}$ to $1300cm^{-1}$, and $1300cm^{-1}$ to $800cm^{-1}$.

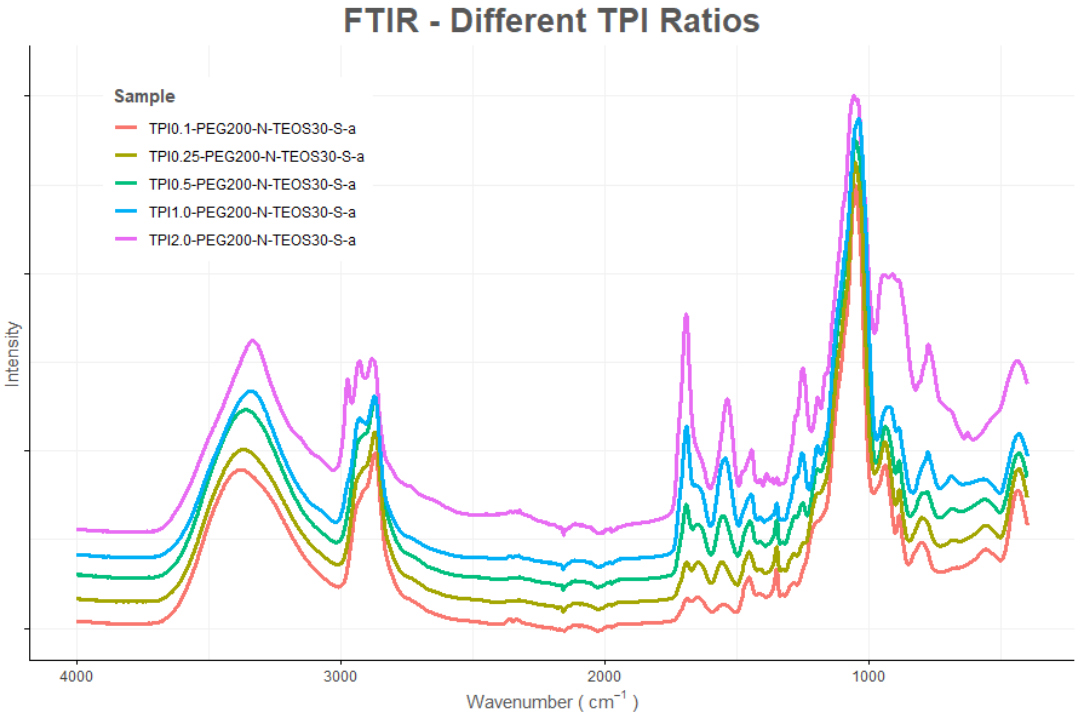

Figure 5.5. Different ratios of TPI, with PEG200 and no catalyst. Each data set is normalized by dividing y values with the max y value, and up shifted by 0.05 in y-axis to make it more visible.

In the $3000cm^{-1}$ to $2750cm^{-1}$ range, on Figure 5.6a, a change in peaks can be observed, where TPI ratio 0.1 has one peak and one shoulder at $2870cm^{-1}$ and TPI ratio 2.0 has three peaks. This wave interval corresponds to $R-CH_3$ and $R-CH_2-R$. Because of the reaction that occurs, a change in the overall composition of the material should not be different from each sample. So the change in FTIR data would indicate that the hybrid material structure becomes different with increasing TPI as the side-chain concentration increases.

The next difference, can be seen on Figure 5.6b, at $1700cm^{-1}$ to $1300cm^{-1}$ where an increase in intensities can be observed. The first peak at $1700cm^{-1}$ would indicate that a $R-COO-R$ group is present, that forms during the reaction between TPI and PEG. However a bump in peak of the data at $1650cm^{-1}$ corresponds to a group of $R-CO-R$, which is a group that forms when TPI reacts with water. So all of the TPI might not have fully reacted with the PEG during the synthesis. At $1550cm^{-1}$ the next peak can be seen, where the intensity also increases with TPI ratio. Because of the increase in intensity, this peak corresponds to the $C-NH-C=O$ group.

It is not possible to determine if TPI has reacted with PEG or water, because it is the $-NH-$ vibrations that are located here. The last peaks in this interval is at $1450cm^{-1}$ and $1350cm^{-1}$, but there is a lot of overlap from the different group and their signals here. So it can be at mix of $R-CH_3$, $R-CH_2-R$ and $R-OH\cdot..O$. If TEOS has not been completely hydrolyzed, the $R-O-CH_2$ group will also appear here.

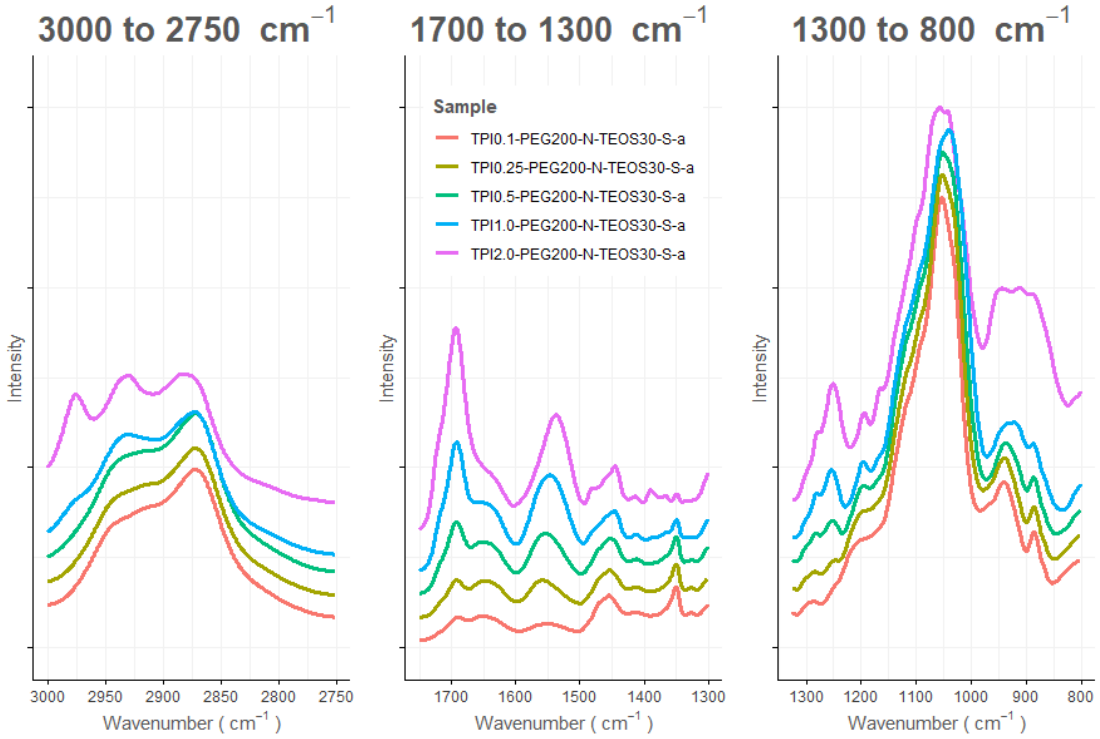

(a) Figure 5.5 in the 2750 to 3000 cm^{-1} range **(b)** Figure 5.5 in the 1700 to 1300 cm^{-1} range **(c)** Figure 5.5 in the 1300 to 800 cm^{-1} range

Figure 5.6. Zoom of different ranges of the FTIR spectra from Figure 5.5, for a clearer view. Each data set is normalized by dividing y values with the max y value, and up shifted by 0.05 in y-axis to make it more visible. The legend is a joined legend for the three zoomed spectra.

In Figure 5.6c the $1300cm^{-1}$ to $800cm^{-1}$ interval is shown. There is a big peak at $1050cm^{-1}$ and some smaller around it, at $1250cm^{-1}$, $1200cm^{-1}$ and $925cm^{-1}$. Again there is some overlap in this region, but because of the reaction mechanism, the big peak must be the SiO_2 network that forms during the aging process. The other peaks are groups of CH_2-O-CH_2, that are in different chemical environments. So the different peaks is the C−O−C asymmetric vibrations that happens at different wavelengths.

The last two peaks that is not mentioned in the regions, where one is a very broad peak at $3300cm^{-1}$, and one at $775cm^{-1}$. The first peak is OH stretching, that can be water that is still trapped in the matrix. There is also a signal from the C−NH−C=O group here and this is also evident from the comparison of the signals with a more narrow peak showing with the increase in TPI ratio. Then the other peak at $775cm^{-1}$ can only come from the SiO_2 network.

5.2.1 Influence of Catalyst in the TPI & PEG Reaction

During the synthesis of the material TPI2.0-PEG200-N-a, an FTIR analysis were performed on the TPI and PEG reaction mixture in the THF solvent after 60 minutes, before any further reagents was added (TPI2.0-PEG200-N-TEOS0-L-a). This showed a prominent peak at $2300cm^{-1}$ on the FTIR, Figure 5.7, and the peak is a standout indicator for the N=C=O bond on the organic reactive end of TPI, suggesting that the TPI and PEG200 had not reacted as intended.

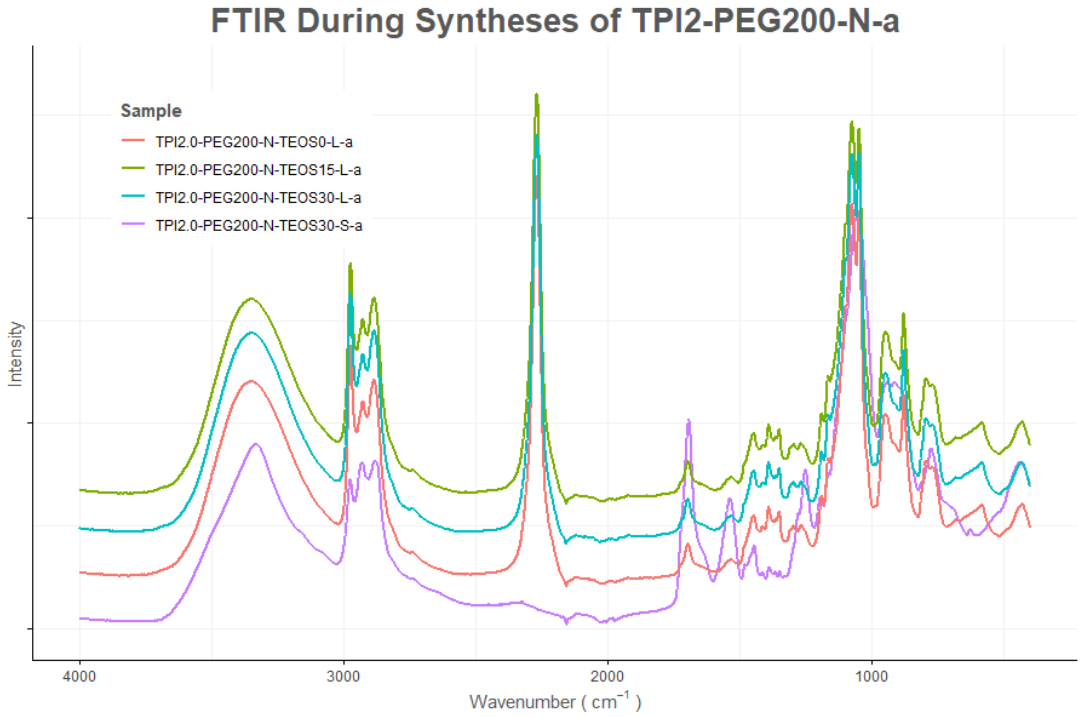

Figure 5.7. FTIR spectra from the syntheses of TPI2-PEG200-N-a. Before the addition of TEOS (TPI2.0-PEG200-N-TEOS0-L-a), 15 minutes after addition of TEOS (TPI2.0-PEG200-N-TEOS15-L-a), 30 minutes after TEOS addition just before starting aging (TPI2.0-PEG200-N-TEOS30-L-a), and after the aging and evaporation process (TPI2.0-PEG200-N-TEOS30-S-a). Each data set is normalized by dividing y values with the max y value, and up shifted by 0.1 in y-axis to make it more visible.

As none of the FTIR spectra of the non-catalyzed solid materials have a peak at this wavenumber, it is clear that the organic end of TPI does react in the expected way. To investigate if the reaction occurred with the addition of the hydrolyzed TEOS, or in the aging and evaporation process. FTIR of TPI2-PEG200-N-a were performed both after 15 minutes (TPI2.0-PEG200-N-TEOS15-L-a) and 30 minutes (TPI2.0-PEG200-N-TEOS30-L-a) of mixing with the hydrolyzed TEOS and these also had a peak at $2300cm^{-1}$. This indicates that isocyanate group on TPI reacts during the aging and evaporation. This is problematic because other unwanted reactions occurs as TPI reacts with the air and water present, during the aging process.

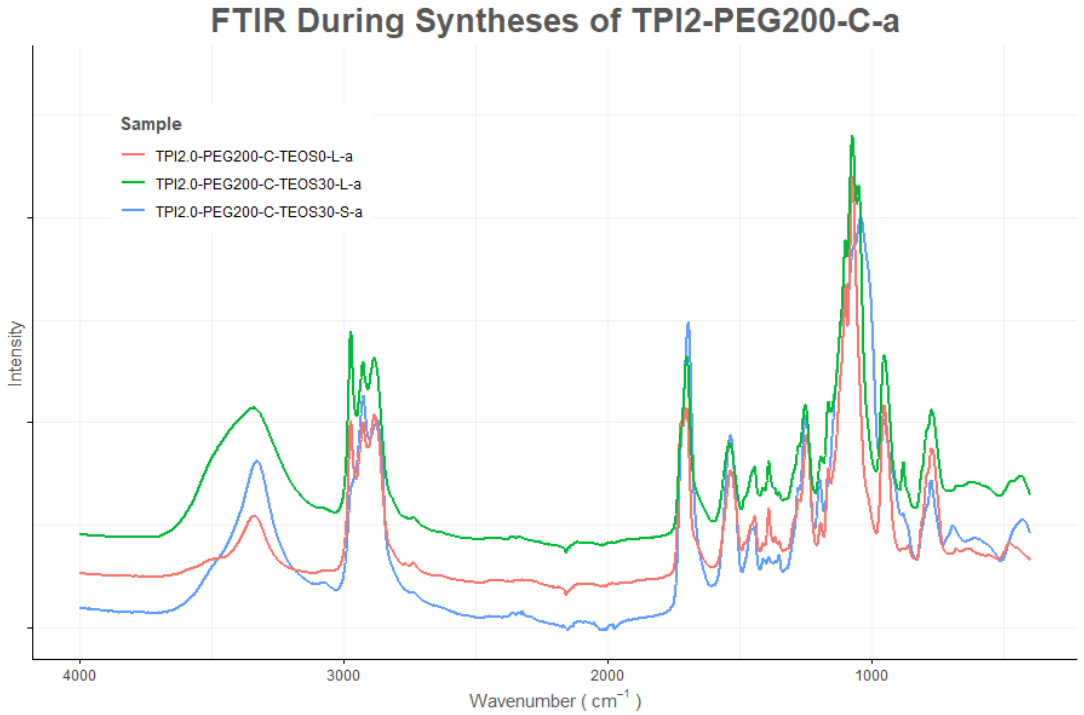

Figure 5.8. FTIR spectra from the syntheses of TPI2-PEG200-C-a. Before the addition of TEOS (TPI2.0-PEG200-C-TEOS0-L-a), 30 minutes after TEOS addition just before starting aging (TPI2.0-PEG200-C-TEOS30-L-a), and after the aging and evaporation process (TPI2.0-PEG200-C-TEOS30-S-a). Each data set is normalized by dividing y values by the max y value, and up shifted by 0.1 in y-axis to make it more visible.

Because of TPI and PEG not reacting as expected, DBTL was added as a catalyst during the reaction of TPI and PEG. FTIR was then performed on the solution TPI2-PEG200-C-a, before the addition of TEOS (TPI2.0-PEG200-C-TEOS0-L-a). Another 30 minutes after mixing with TEOS(TPI2.0-PEG200-C-TEOS30-L-a), and lastly also of the solid material (TPI2.0-PEG200-C-TEOS30-S-a) (see Figure 5.8). They show no peak at $2300cm^{-1}$ after the initial TPI and PEG mixing, indicating they have had the desired reaction. The peak at $1700cm^{-1}$ that in the non-catalyzed solid material had a little bump, seems to be mostly gone when using catalyst.

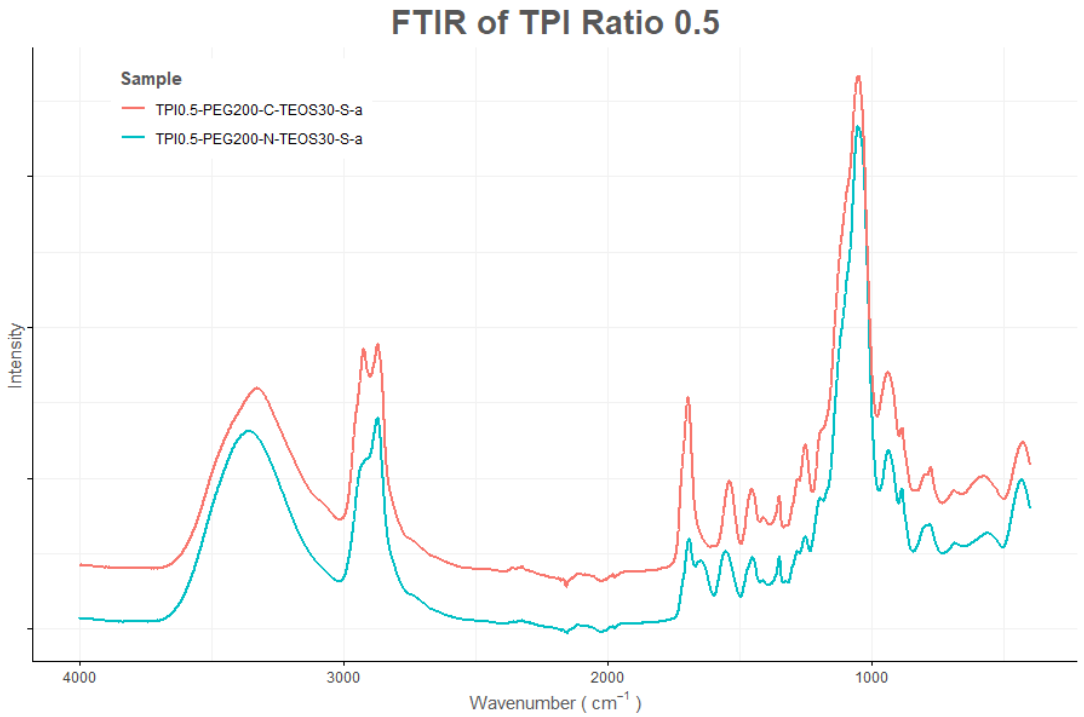

Figure 5.9. Spectra comparison of the ratio 0.5 TPI coupling agent, blue line is the non catalyzed (TPI0.5-PEG200-N-TEOS30-S-a), and orange is the catalyzed material (TPI0.5-PEG200-C-TEOS30-S-a). Each data set is normalized by dividing y values with the max y value, and up shifted by 0.1 in y-axis to make it more visible.

The spectra do not have the R−CO−R group and therefore the undesired reaction with water has been avoided. For a better comparison of the differences between catalyzed and non-catalyzed see Figure 5.9 that shows the two scenarios for the 0.5 TPI ratio. Besides not having the peak for R−CO−R, another peak at $1200cm^{-1}$ seems to be gone or at least shifted. This peak is where the CH_2-O-CH_2 group is located, as this group is present in PEG, a change in the chemical environment might be to blame. Other increases in peak intensities is considered to be from the addition of the catalyst within the hybrid glass.

To understand whether the DBTL catalyst influences the hybrid sol-gel at different ratios of TPI, the corresponding FTIR data are compared, as shown in Figure 5.10a. Evaluation of the FTIR spectra showed many of the same bonds present in non-catalyzed material (Figure 5.2), is also present in catalyzed material. The most noticeable differences found in the $1700cm^{-1}$ and $1550cm^{-1}$ (Figure 5.10b). Here the spectra of the TPI ratio 2.0 and 3.0, are similar and it appears that the catalyst is effective.

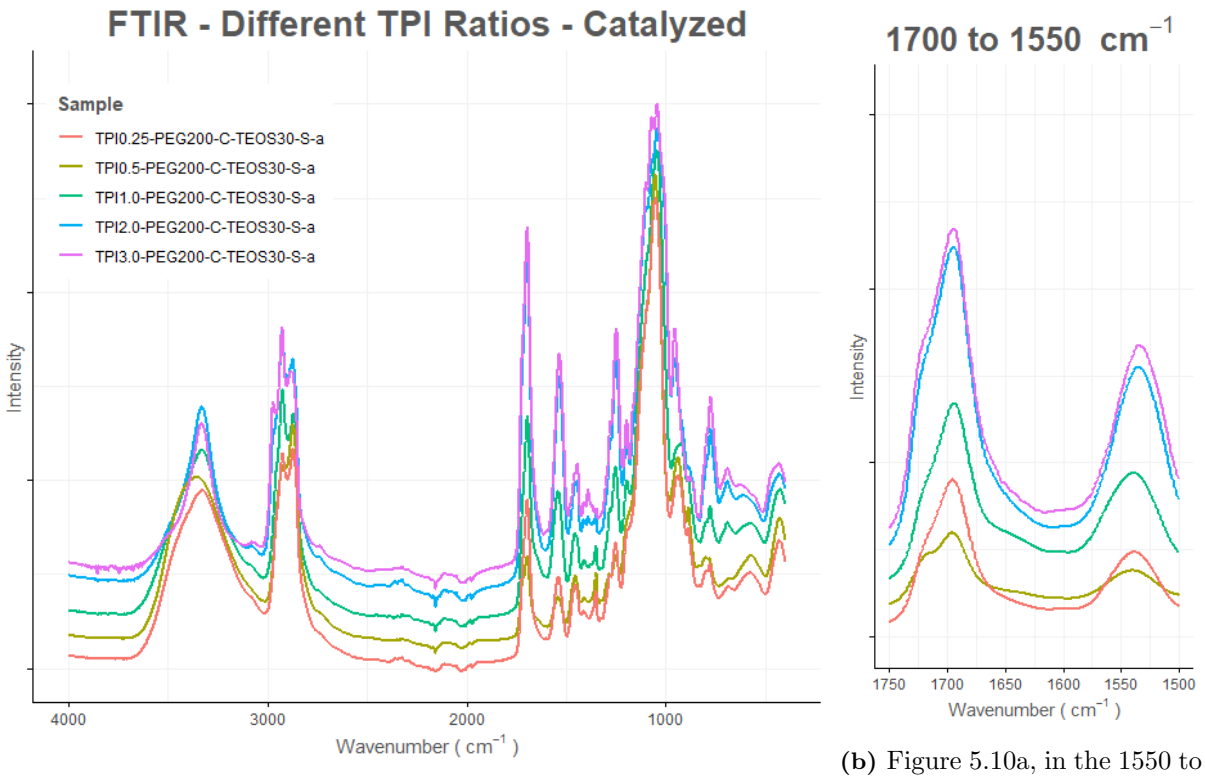

(a) Different ratios of TPI, with PEG200 catalyzed by DBTL.

(b) Figure 5.10a, in the 1550 to 1700 cm^{-1} interval

Figure 5.10. Both data set is normalized, by dividing y values with the max y value, and up shifted by 0.05 in y-axis to make it more visible. The legend is a joined legend for both spectra.

Beside the indication that ratio 2.0 and 3.0 appears to be similar, FTIR of these samples after the catalyzed reaction between PEG and TPI (Figure 5.11), showed a clear peak at 2300 cm^{-1}, for the 3.0 ratio. As explained in Section 5.2.1 a peak at 2300 cm^{-1} indicates that all TPI have not reacted with PEG. Remaining TPI is expected as the theoretical ideal ratio is 2-TPI:1-PEG. Remaining TPI will have unwanted reactions. Therefore, a ratio of 2.0 is better to continue experimenting on.

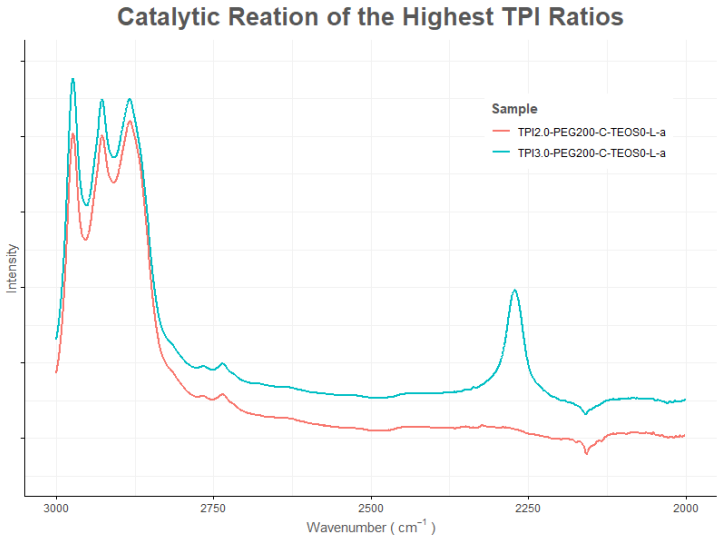

Figure 5.11. FTIR analysis of the molar ratio 2.0 (TPI2.0-PEG200-C-TEOS0-L-a) and ratio 3.0 (TPI3.0-PEG200-C-TEOS0-L-a) sol after the catalytic reaction of PEG and TPI, before addition of TEOS. Both data set is normalized, by dividing y values with the max y value, and up shifted by 0.05 in y-axis to make it more visible.

5.3 Performance of Synthesized Materials

5.3.1 Qualitative Assessment of Key Material Aspects

Table 5.1. Table of the values given from a scale 1-5 of different proprieties of the materials, through a qualitative evaluation of the hybrid material. Data for all hybrid materials can be found in Table E.1.

Material	Transparency	Firmness	Flexibility	Toughness	Surface	Sum
TPI1.0-PEG200-N-TEOS30-S-a	5	5	2	4	5	21
TPI0.5-PEG200-N-TEOS30-S-a	5	5	2	4	5	22
TPI0.25-PEG200-N-TEOS30-S-a	4	5	1	4	5	19
TPI2.0-PEG200-N-TEOS30-S-a	4	2	3	4	4	17
TPI1.0-PEG200-C-TEOS30-S-a	4	5	2	3	4	18
TPI2.0-PEG200-C-TEOS30-S-a	4	5	3	5	4	21
TPI0.5-PEG200-C-TEOS30-S-a	4	3	3	3	4	17
TPI0.25-PEG200-C-TEOS30-S-a	5	3	2	2	4	16

Table 5.1 shows the values given in the qualitative assessment of the materials with a TPI ratio of 0.25-2.0 catalyzed and non-catalyzed.

The sum of individual scores indicates how the material performs overall, however, it is important to look at the individual factors as flexibility and toughness are more important parameters for the aim of the report. So TPI0.5-PEG200-N-TEOS30-S-a has the highest sum-score but, TPI2.0-PEG200-C-TEOS30-S-a perform better in the important parameters, indicating it would be the better candidate for continued work with this material.

5.3.2 Water Stability Comparison of the Non-catalyzed & Catalyzed TPI Ratios

For a better understanding of the hybrid material and how interconnected it is. The samples was submerged in water and then dried. If the weight loss is low after the drying, then it is expected to be bond together by covalent bonds. Then the coupling agent has worked as intended, See Figure 5.12.

Table 5.2. The data from the water experiment performed.

Material	Weight Start	Weight End	Diff.	W/W Diff.
TPI0.1-PEG200-N-TEOS30-S-a	0.1237	0.0465	-0.0772	-62.41%
TPI0.25-PEG200-N-TEOS30-S-a	0.2830	0.1345	-0.1485	-52.47%
TPI0.5-PEG200-N-TEOS30-S-a	0.2543	0.1512	-0.1031	-40.54%
TPI1.0-PEG200-N-TEOS30-S-a	0.2199	0.1279	-0.092	-41.84%
TPI2.0-PEG200-N-TEOS30-S-a	0.2303	0.1264	-0.1039	-45.12%
TPI0.25-PEG200-C-TEOS30-S-a	0.2596	0.1286	-0,1310	-50,46%
TPI0.5-PEG200-C-TEOS30-S-a	0.1285	0.0912	-0.0373	-29.03%
TPI1.0-PEG200-C-TEOS30-S-a	0.4690	0.3767	-0.1485	-19.68%
TPI2.0-PEG200-C-TEOS30-S-a	0.1266	0.1199	-0.0067	-5.29%

The experiment showed that a catalyzed PEG200 material, lost less weight with a higher TPI ratio. The low TPI ratio of 0.25 lost about 50% mass, and the high TPI ratio of 2.0 lost around 5% mass. For the non-catalyzed counterpart, the low ratio TPI 0.25 lost about 50% and the high lost 45%. The increased water stability of the catalyzed material, indicates that the components used are bond in the structure.

For the non-catalyzed reaction the material with lowest mass loss has a TPI ratio of 0.5. There is no correlation with increase in TPI and less mass loss. However, the catalyzed materials showed better water stability with higher TPI ratio. This could indicate that a 60-minute reaction time for the TPI and PEG mix is sufficient for a TPI ratio of 0.5, but not for higher TPI ratios.

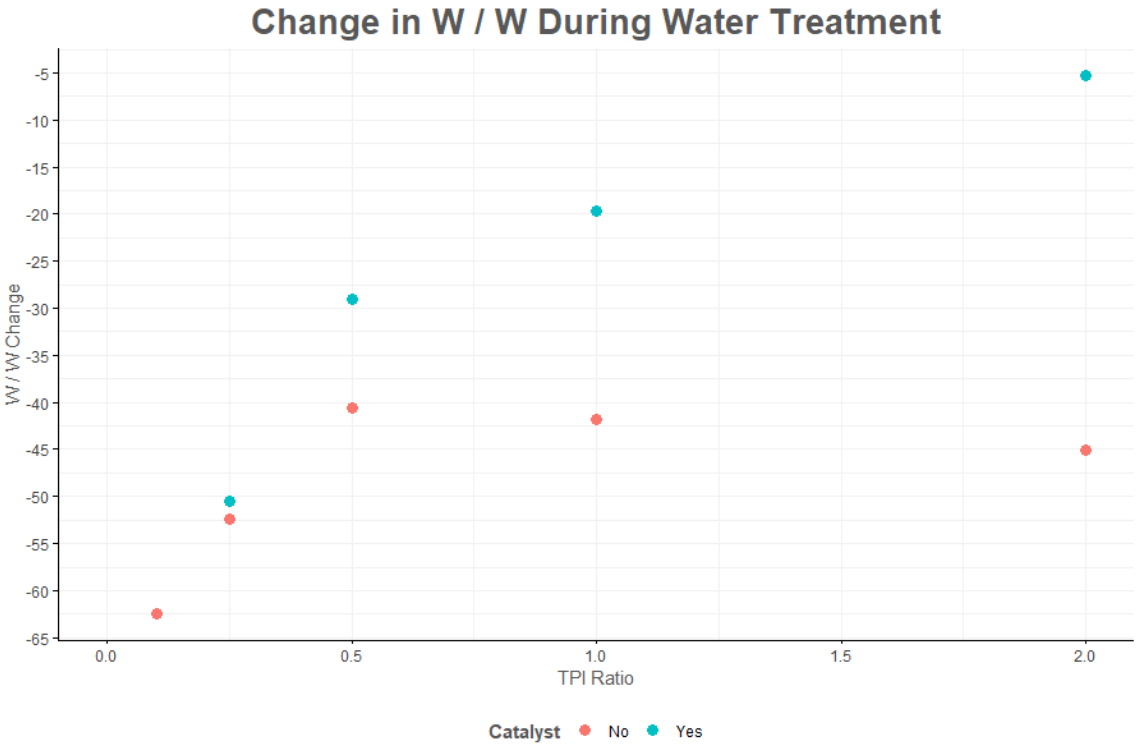

Figure 5.12. Graph of the mass change depending on the TPI ratio in the material. The negative W/W Change means mass is lost

Chemical structure after water treatment

In Section D.1 pictures of the samples after water treatment can de seen, in general all the materials acquired small cracks, lowering the transparency, and toughness of the material.

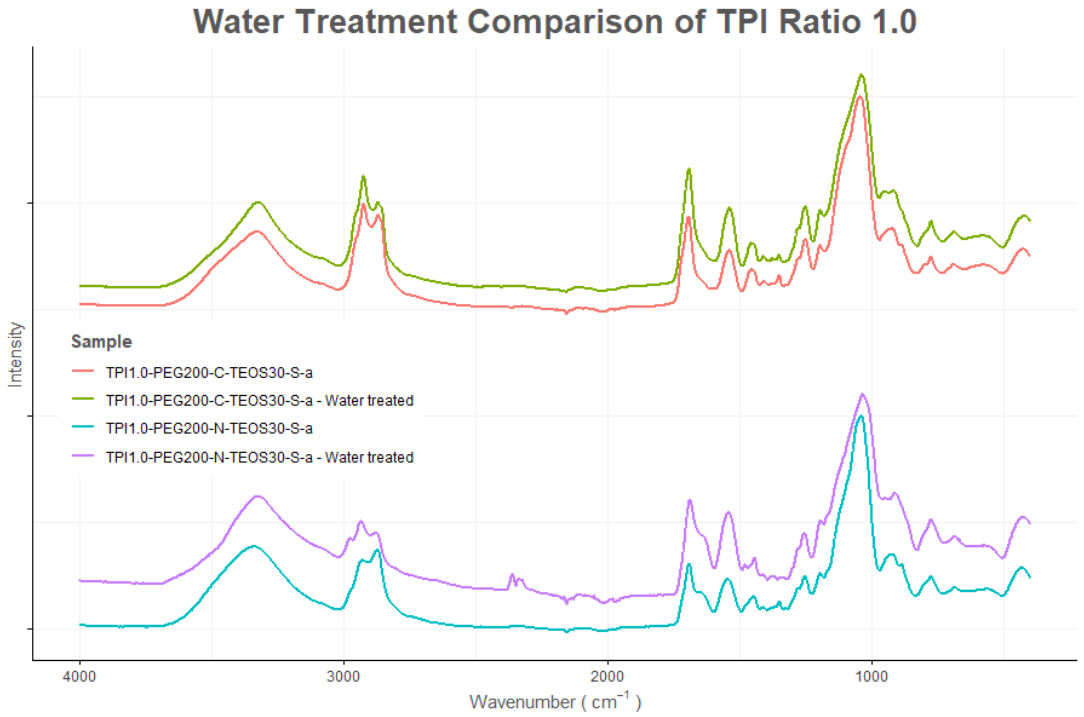

Figure 5.13. Comparison of TPI ratio 1.0 with catalyst (TPI1.0-PEG200-C-TEOS30-S-a) and without (TPI1.0-PEG200-N-TEOS30-S-a), before and after water treatment. Each data set is normalized, by dividing y values with the max y value. Spectra is up-shifted by 0.1 with there partner and by 1.5 by groups for better visualization.

FTIR was measured on the water treated samples. The spectra for all the samples can be found in Appendix D.2. In Figure 5.13 two examples of the treatment are pictured. The top sample is the catalyzed 1.0 TPI ratio material. There are no noticeable differences before and after treatment which indicates that the 19.68% weight loss are not part of the structure, detectable by FTIR.

The bottom example is the non-catalyzed version of the TPI 1.0 ratio. Here, it can be seen that the peaks at $\approx 2900 cm^{-1}$ change along with peaks in the 1300 to 1500 cm^{-1} range. The change in the FTIR indicates that non-catalyzed materials exhibit a change in chemical environment and structure, as components contributing to the structure are washed out during the water treatment. This could be TPI and PEG bonded by intermolecular forces.

5.3.3 Thermal Stability Comparison of the Non-catalyzed & Catalyzed TPI Ratios Using TGA Results

From the TGA in Figure 5.14, it is visible that there is a slow release of possible water molecules that are adsorbed between 0 to 200°C. It can also be other volatile residues of either ethanol or THF. Around the 200°C a significant weight loss is recorded, which could be the flash point of free PEG. From here the organic matter is released as the polymer breaks down and is seen as the rapid drop when heating past 200 °C. However, When comparing the non-catalyzed to the catalyzed samples, it is evident that the mass change in the catalyzed samples is not as large as in the non-catalyzed ones, although it still occurs. This can indicate the network is better interconnected and results in better overall thermal stability of the material. Then another accelerated weight loss occurs in the 400°C region. This indicates a further release of other strongly bonded organic sites, which could be closer bonded to the silica network [11].

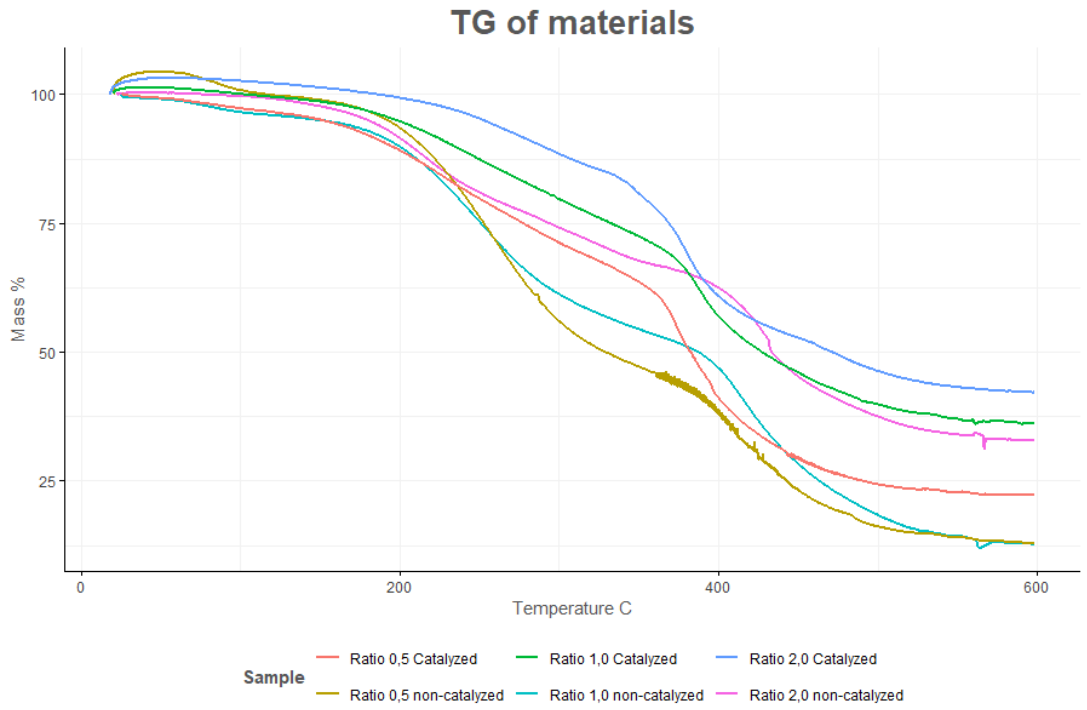

Figure 5.14. Graph of TGA data of the different ratios; both non-catalyzed and catalyzed hybrid sol-gel materials, x-axis is the temperature, and y-axis is the mass loss in percent.

Overall, when comparing the non-catalyzed and catalyzed, the difference is increased thermal stability in the catalyzed materials. The weight loss is also reduced in the 200-400°C region. This indicates that the polymer might be better bonded to the silica network, which is also the seen in a published article working with similar materials [11]. Also it is visible that by increasing the TPI ratio, it will increase the thermal stability. This is also validated when comparing the non-catalyzed to each other.

Conclusion 6

TPI was used as a coupling agent to make a stable hybrid material by acting as a bridge connecting TEOS and PEG. This was carried out in different ratios and with or without DBTL as catalyst.

FTIR analysis of the synthesized materials, verified that the materials were combined in a non-brittle matrix. The desired reaction between TPI and PEG did not fully occur, as the standout FTIR peak for the N=C=O bond from TPI, was still present before the addition of TEOS. DBTL was added as a catalyst to enhance the desired reaction between TPI and PEG. A confirmation of the reaction was obtained by FTIR.

The TGA analysis shows that TPI2.0-PEG200-C-TEOS30-S-a has the smallest loss of mass and thereby is more covalently bonded in the hybrid matrix. This is further verified by the water experiment. Here the hybrid materials were submerged in water and excess water was removed afterwards. TPI2.0-PEG200-C-TEOS30-S-a had the smallest loss of mass of -5,29 W/W%, which is better compared to the rest of the hybrid materials, thus showing a better water stability.

Qualitative assessment of the firmness, flexibility, toughness, and surface was used to determine the performance of the synthesized materials. It was revealed that TPI2.0-PEG200-C-TEOS30-S-a, had one of the best overall assessments. The FTIRs that showed this material to have a more fulfilled reaction of the TPI and PEG bonding. Combining this with the Thermogravimetric Analysis and water treatment results, it is concluded that TPI2.0-PEG200-C-TEOS30-S-a exhibits improved covalent bonding, making it the most stable and flexible hybrid material produced.

Further Research 7

Working with the TEOS, TPI, and PEG system requires further testing. Experiments could include further optimizing of various parameters, such as the polymer size to a larger average molar mass (M_n), adjusting the ratio of TEOS to PEG.

Some experiments with a larger average molar mass were performed. These were syntheses with catalyzed PEG-400, 600, and 1000 Da. TPI0.5-PEG400-C-TEOS30-S-a showed an increase in flexibility compared to the results from PEG-200. PEG-600 showed some of the most promising results in terms of flexibility yet, with close to a 100°sustained bend. While PEG-1000 became brittle and visually appears crystalline. Due to low sample size and no consistent analyses, these were not presented in the report, however they can be seen in Appendix C.

Mechanical testing of the materials from this report and possible future materials should be performed, to give a quantitative approach with data describing the material objectively. The test could be a controlled drop test, Vickers Hardness, and a quantitative Flexibility test.

The sol-gel hybrid materials developed for this report did not prioritize material thickness, which could significantly impact the overall flexibility. Assuming the material is made thinner, it would likely perform better in terms of flexibility. This is similar to the ultra-thin materials used in the current generation of Samsung Galaxy Flip phones, despite being composed of hard oxide material their thickness contributes to their flexibility.

Because of the time constrains of the project the use of catalyst was necessary to react the PEG with TPI. This could possibly be omitted if the reaction was done for a longer period of time, or by increasing the temperature of the mix.

As the sol-gel process is a liquid product before aging, it could be used as a coating layer for other already flexible materials. With this approach it can be tested how much a coating layer of the sol-gel material would improve the hardness of the flexible TPU film, while testing the impact on flexibility by adding a more rigid layer on top.

Bibliography

[1] R. Dsouza, "What do american consumers do when their phone screens crack?," tech. rep., Jan. 31st -2024. https://business.yougov.com/content/48503-what-do-american-consumers-do-when-their-phone-screens-crack, read d. 04-11-2024.

[2] Rachel Jefferies, *3 Types of Screen Protectors: Pros & Cons.* https://screenshield.com.au/blogs/blog/pros-and-cons-of-screen-protectors?srsltid=AfmBOoqXf69dOpuEsi05MAGe1qAOV7PeyW2D_ESOezlPvXx78hYxaEQo, Jun 2022. read d. 29-11-2024.

[3] Joe Maring, *A (brief) history of the folding phone.* https://www.androidcentral.com/brief-history-folding-phone, May 2021. read d. 23-09-2024.

[4] John Awa-abuon, *How Do Foldable Smartphone Screens Actually Work?* https://www.makeuseof.com/how-do-foldable-smartphone-screens-actually-work/, Jun 2021. read d. 23-09-2024.

[5] Bogdan Petrovan, *How do folding screens actually work?* https://www.androidauthority.com/how-do-folding-screens-actually-work-3164822/, Sep. 2023. read d. 25-11-2024.

[6] Renee Christian, *How much will replacing the Samsung Galaxy Z Flip 5 screen cost?* https://www.androidpolice.com/samsung-galaxy-z-flip-5-screen-replacement-cost/, Aug 2023. read d. 27-09-2024.

[7] Hadlee Simons, *How much does it cost to replace a foldable phone's screen?* https://www.androidauthority.com/foldable-phone-screen-repair-costs-1069279/, Aug 2023. read d. 29-11-2024.

[8] Torras, *TPU vs Tempered Glass Screen Protectors: Which Should You Choose?* https://torraslife.com/blogs/all/tpu-vs-tempered-glass-screen-protectors-which-should-you-choose, Jun 2024. read d. 29-11-2024.

[9] E. Burunkaya, Ömer Kesmez, N. Kiraz, H. E. Çamurlu, M. Çamurlu, and E. Arpaç, "Hydrophilic hybrid sio2: Polyethylene glycol-3-isocyanato- propyltrietoxysilane nanocomposite films," *Thin solid films, Vol.522*, pp. p.238–246, 2012. DOI: 10.1016/j.tsf.2012.08.038.

[10] Y. Zhang, Z. Chen, H. Zheng, R. Chen, C. feng Ma, and G. Zhang, "Multifunctional hard yet flexible coatings fabricated using a universal step-by-step strategy," *Advanced science, Vol.9 (14)9,2200268*, pp. p.1–10, 2022. DOI: 10.1002/advs.202200268.

[11] C. Oh, Y.-G. Lee, T.-S. Choi, C.-U. Jon, and S.-G. Oh, "Facile synthesis of peg–silica hybrid particles using one-step sol–gel reaction in aqueous solution," *Colloids and Surfaces A: Physicochemical and Engineering Aspects*, vol. 349, no. 1, pp. 145–150, 2009.

[12] P. M. E. Q. C. T. L. M. S. Grandi, A. Magistris, "Synthesis and characterization of sio2–peg hybrid materials," *Journal of Non-Crystalline Solids*, pp. Page 273–280, 2006. https://doi.org/10.1016/j.jnoncrysol.2005.11.033, read d. 27-11-2024.

[13] J. I. Gersten and F. W. Smith, *The PHYSICS and CHEMISTRY of MATERIALS*. John Wiley & Sons, INC., 2001. ISBN:0-471-05794-0, pp. 790-795, read d. 28-09-2024.

[14] A. M. E. Nahrawy, *Egyptian Journal of Chemistry Vol. 65.* No. 11, NIDOC, 2022. https://journals.ekb.eg/article_223473.html, read d. 13-12-2024.

[15] A. A. E. P. D. F. C.-E. S. Woignier T, Primera J, "Mechanical properties and brittle behavior of silica aerogels.," *Gels*, pp. Page 256–275, 2015, 1(2). https://doi.org/10.3390/gels1020256, read d. 27-11-2024.

[16] M. M. K. Michel A. Aegerter, Nicholas Leventis, *Aerogels Handbook*. Springer New York, NY, 2011. https://doi.org/10.1007/978-1-4419-7589-8, read d. 20-11-2024.

[17] K. Baskaran, M. Ali, K. Gingrich, D. L. Porter, S. Chong, B. J. Riley, C. W. Peak, S. E. Naleway, I. Zharov, and K. Carlson, "Sol-gel derived silica: A review of polymer-tailored properties for energy and environmental applications," *Microporous and Mesoporous Materials*, vol. 336, p. 111874, 2022.

[18] B. M. Novak, "Hybrid nanocomposite materials—between inorganic glasses and organic polymers," *Advanced Materials*, vol. 5, no. 6, pp. 422–433, 1993.

[19] L. M. Polgar and et al., "Influence of the chemical structure of cross-linking agents on properties of thermally reversible networks," *Pure and Applied Chemisty*, p. vol 88 issue 12, 2016. https://www.degruyter.com/document/doi/10.1515/pac-2016-0804/html, read d. 07-11-2024.

[20] N. Abidi, *FTIR Microspectroscopy: Selected Emerging Applications. 1st edition.* Springer Nature Switzerland AG 2021, 2022. ISBN; 978-3-030-84426-4.

[21] Bruker, "Guide to infrared spectroscopy." https://www.bruker.com/en/products-and-solutions/infrared-and-raman/ft-ir-routine-spectrometer/what-is-ft-ir-spectroscopy.html, read d. 01-10-2024.

[22] J.-M. Ruysschaert and V. Raussens, *ATR-FTIR analysis of amyloid proteins*, vol. 1777, pp. 69–81. 05 2018.

[23] G. Raspoet, M. T. Nguyen, M. McGarraghy, and A. F. Hegarty, "The alcoholysis reaction of isocyanates giving urethanes: Evidence for a multimolecular mechanism," *The journal of organic chemistry*, vol. 63, no. 20, pp. 6878–6885, 1998.

[24] P. J. Larkin, *Infrared and Raman spectroscopy: principles and spectral interpretation. 2nd edition.* Elsevier, 2018. ISBN; 978-0-12-804162-8.

[25] A. C. Hernández-González, L. Téllez-Jurado, and L. M. Rodríguez-Lorenzob, "Synthesis of in-situ silica-alginate hybrid hydrogels by a sol gel route," *Carbohydrate polymers, Vol.250, Article 116877*, pp. p.116877–116877, 2020. DOI: 10.1016/j.carbpol.2020.116877.

[26] W. Fan, T. Du, A. Droce, L. R. Jensen, R. E. Youngman, X. Ren, L. Gurevich, M. Bauchy, P. Kristensen, and B. Xing, "Resolving the conflict between strength and toughness in bioactive silicapolymer hybrid materials," *ACS Nano, vol. 16 (6)*, pp. p. 9748–9761, 2022. DOI: 10.1021/acsnano.2c03440.

Estimate of Wavenumber A

Table A.1. A generalized estimate of which wavenumber ($[cm^{-1}]$) each functional group has [24]. Here *asym* is asymmetric, *sym* is symmetric, *str* is stretch, *bend* is bending and *wag* is wagging.

Functional Group	Wave number	Vibration type	IR intensity	Raman intensity
$R-OH....O$	3400-3200	OH str	s br.	vw
	1420-1390	OH bend	w	-
	800-600	OH wag	m br.	-
$R-COO-R$	1750-1735	C=O str	s	m
$R-CH_3$	2975-2950	asym str	vs	vs
	2885-2860	sym str	vs	vs
	1470-1440	asym bend	ms	ms
	1380-1370	sym bend	m	vw
$C-NH-C=O$	3320-3270	NH str	ms	w
	1570-1515	CNH str bend	ms	w
$R-CH_2-R$	2936-2915	asym str	vs	vs
	2865-2833	sym str	vs	vs
	2920-2890	Fermi Resonance	w	m
	1445-1475	bend	ms	ms
$R-NCO$	2300-2250	NCO asym str	vs	vw
CH_2-O-CH_2	1270-1060	COC asym str	s	w
	1140-800	COC sym str	m	s
$Si-O$	1100-1000	Si-O str	vs	w
$(-SiO_2-)_x$	1100	-	vs	-
	470	-	m	-
CH_2-OH	1090-1000	C-O str	s	mw
	900-800	C-O str	mw	s
Epoxy	1270-1245	ring sym str	m	s
	935-830	ring asym str	s	m
$R-O-CH_2$	1390-1340	wag	m	m
$R-O-CH_3$	2850-2815	sym str	m	m
	1450-1430	sym bend	ms	m
$R-CO-R$	1725-1705	C=O str	s	m

Pictures of Synthesized Hybrid Materials

B

TPI ratio: 0.25 without catalyst
TPI0.25-PEG200-N-TEOS30-S-a

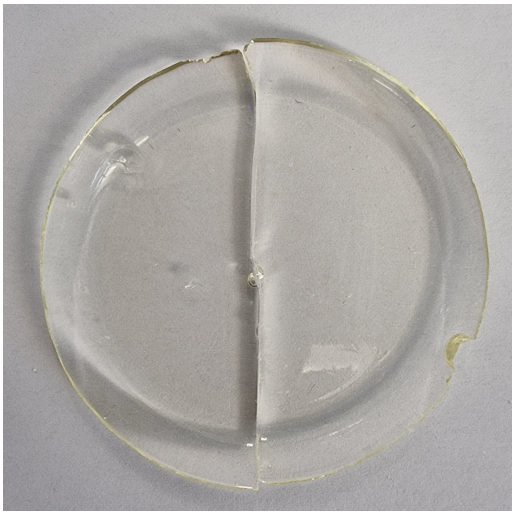

TPI ratio: 0.25 With Catalyst
TPI0.25-PEG200-C-TEOS30-S-a

TPI ratio: 0.5 without catalyst
TPI0.5-PEG200-N-TEOS30-S-a

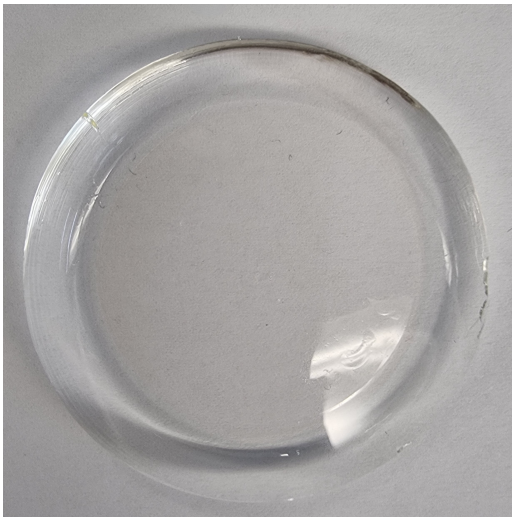

TPI ratio: 0.5 With Catalyst
TPI0.5-PEG200-C-TEOS30-S-a

TPI ratio: 1.0 without catalyst
TPI1.0-PEG200-N-TEOS30-S-a

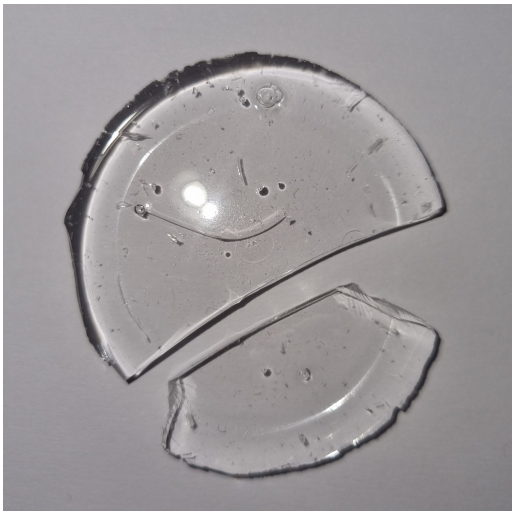

TPI ratio: 1.0 With Catalyst
TPI1.0-PEG200-C-TEOS30-S-a

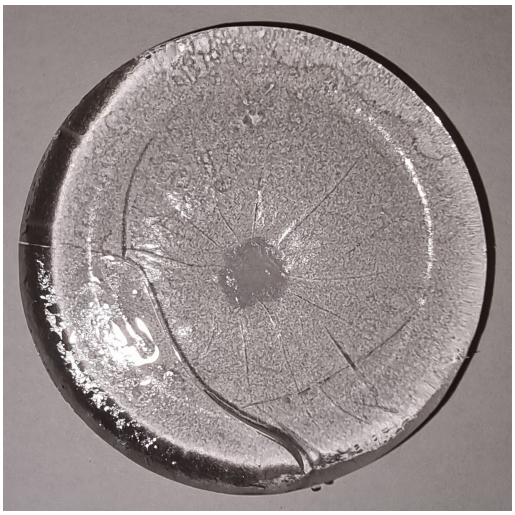

TPI ratio: 2.0 without catalyst
TPI2.0-PEG200-N-TEOS30-S-a

TPI ratio: 2.0 With Catalyst
TPI2.0-PEG200-C-TEOS30-S-a

TPI ratio: 0.1 without catalyst
TPI0.1-PEG200-N-TEOS30-S-a

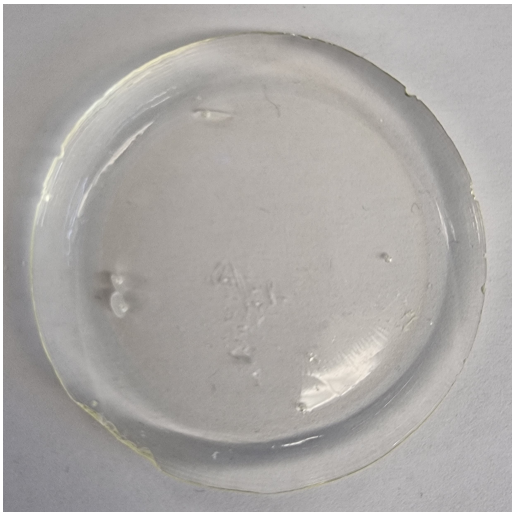

TPI ratio: 3.0 With Catalyst
TPI3.0-PEG200-C-TEOS30-S-a

Pictures of Synthesized Hybrid Materials with Other PEG M_n

C

TPI0.5-PEG400-C-TEOS30-S-a

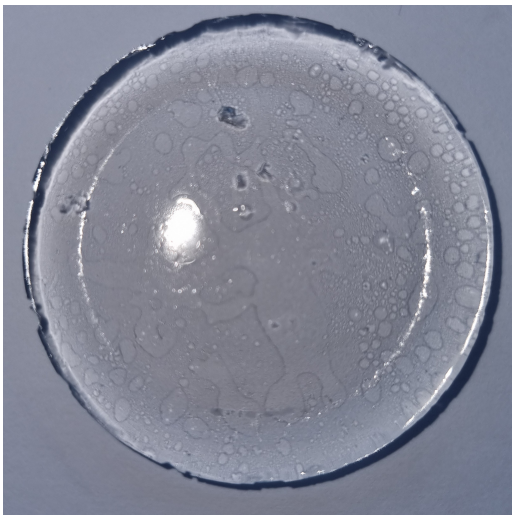

TPI0.5-PEG400-C-TEOS30-S-a bend

TPI0.33-PEG600-C-TEOS30-S-a

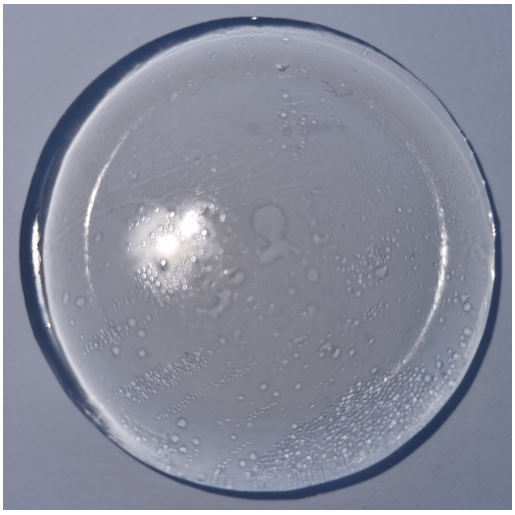

TPI0.33-PEG600-C-TEOS30-S-a Bend

TPI0.2-PEG1000-C-TEOS30-S-a	TPI0.2-PEG1000-C-TEOS30-S-a bend
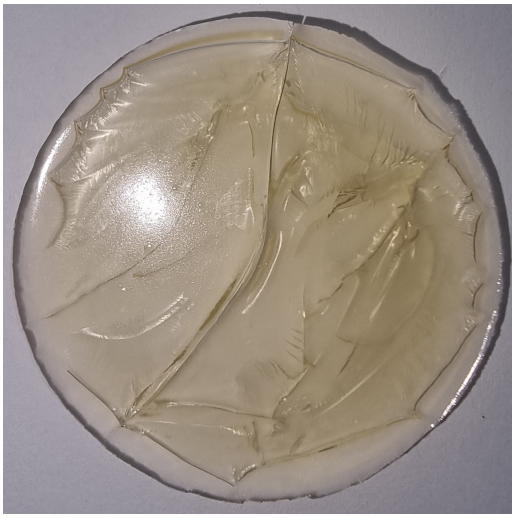	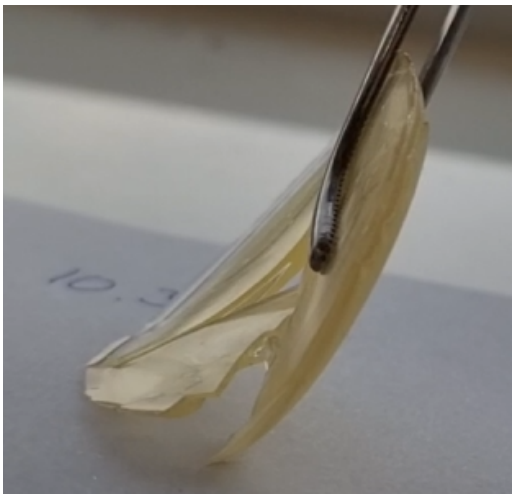

After Water Treatment D

D.1 Pictures

TPI ratio: 0.25 without catalyst
TPI0.25-PEG200-N-TEOS30-S-a

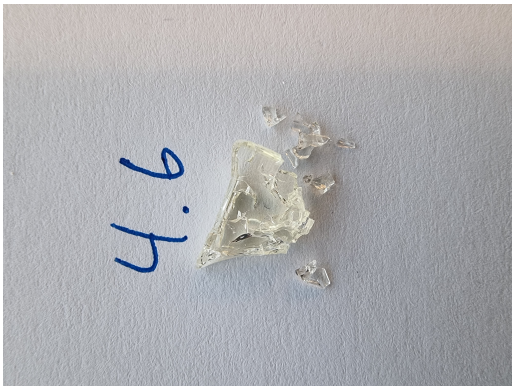

TPI ratio: 0.25 With Catalyst
TPI0.25-PEG200-C-TEOS30-S-a

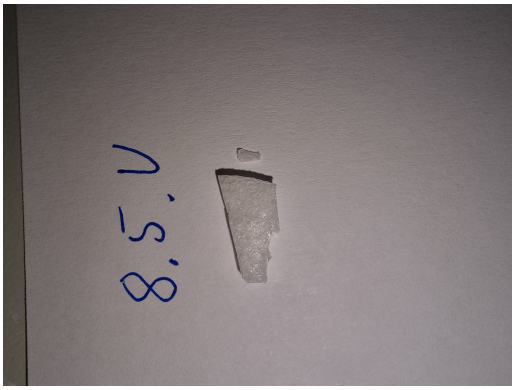

TPI ratio: 0.5 without catalyst
TPI0.5-PEG200-N-TEOS30-S-a

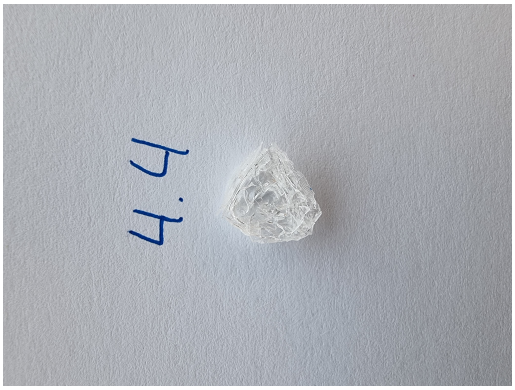

TPI ratio: 0.5 With Catalyst
TPI0.5-PEG200-C-TEOS30-S-a

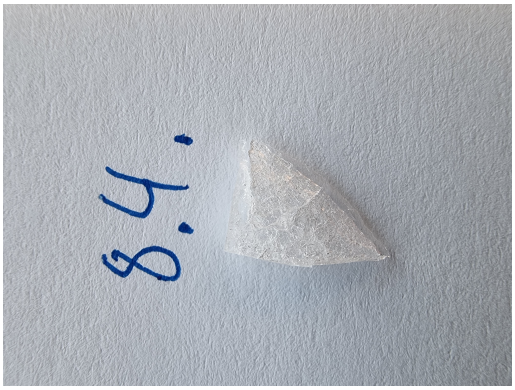

TPI ratio: 1.0 without catalyst TPI1.0-PEG200-N-TEOS30-S-a 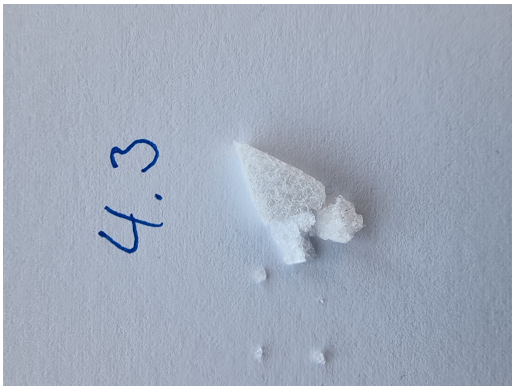	TPI ratio: 1.0 With Catalyst TPI1.0-PEG200-C-TEOS30-S-a 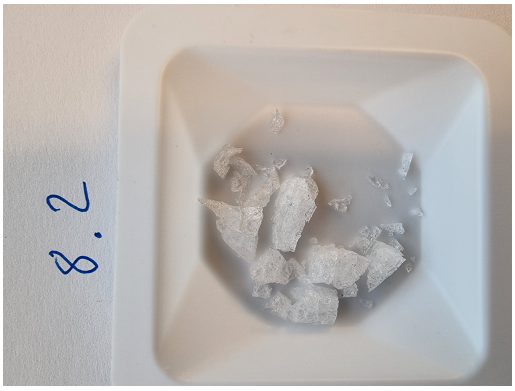
TPI ratio: 2.0 without catalyst TPI2.0-PEG200-N-TEOS30-S-a 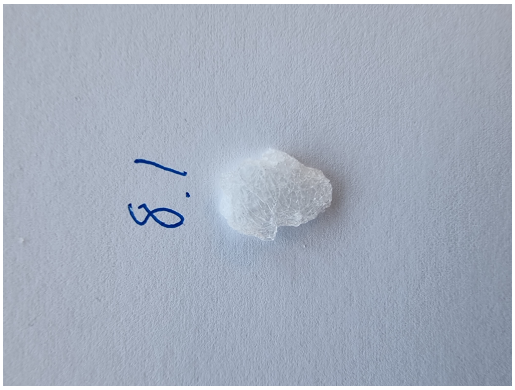	TPI ratio: 2.0 With Catalyst TPI2.0-PEG200-C-TEOS30-S-a 
TPI ratio: 0.1 without catalyst TPI0.1-PEG200-N-TEOS30-S-a 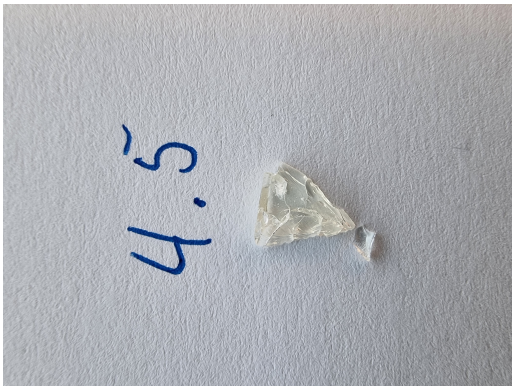	

D.2 FTIR

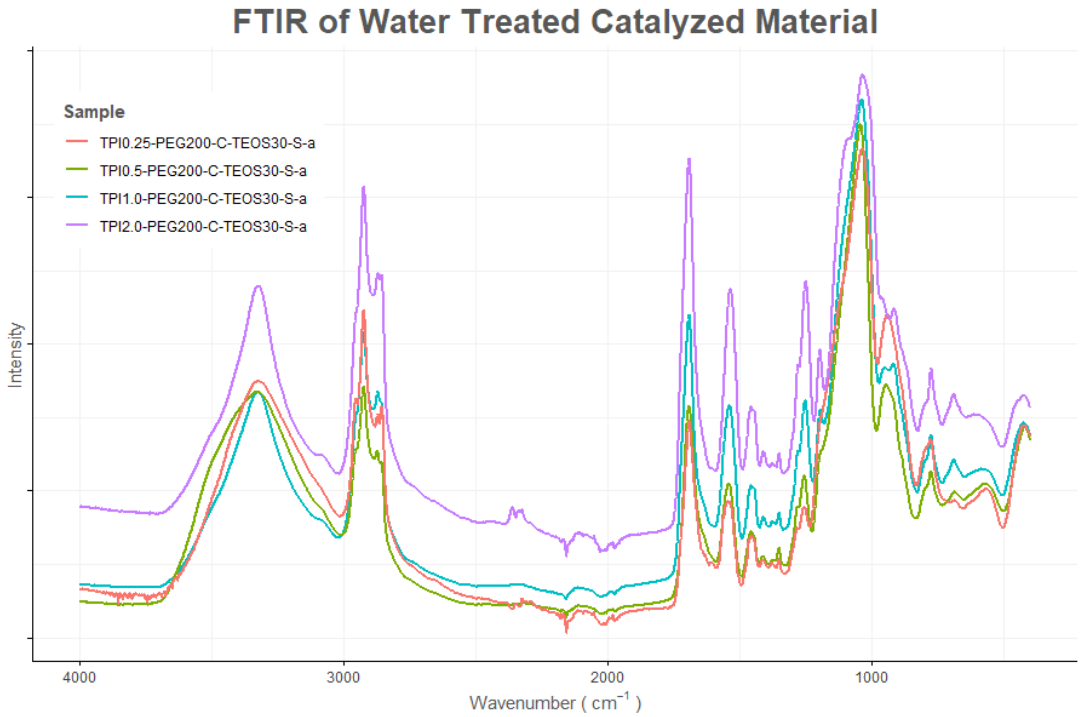

Figure D.1. FTIR for water treated catalyzed samples. Each data set is normalized by dividing y values by the max y value, and up shifted by 0.05 in y-axis to make it more visible.

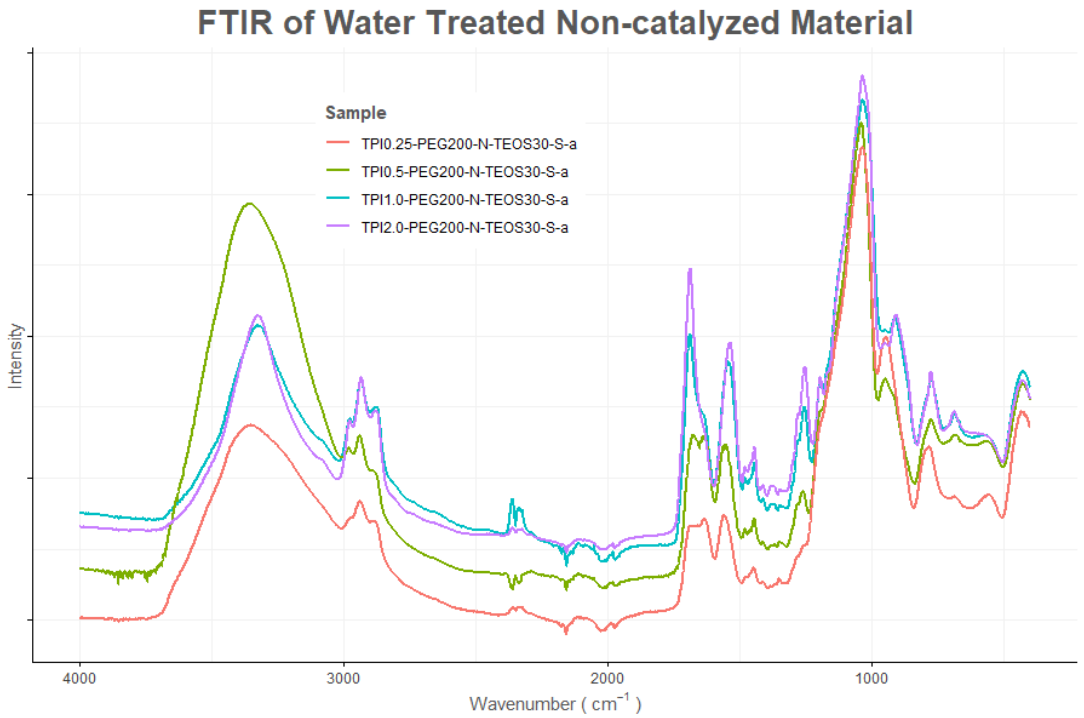

Figure D.2. FTIR for water treated catalyzed samples. Each data set is normalized by dividing y values by the max y value, and up shifted by 0.05 in y-axis to make it more visible. Difference is found in TPI0.5-PEG200-N-TEOS30-S-a in the range 3000-3750 cm^{-1}

Performance Rating of Materials

E

Table E.1. Table of the values given from a scale 1-5 of different proprieties of the materials, though a physichal inspection of the material.

Material	Transparency	Firmness	Flexibility	Toughness	Surface	Sum
GPTMS0.25-PEG200-N-TEOS60-S-a	5	3	2	1	5	16
GPTMS0.25-PEG200-N-TEOS60-S-b	4	3	1	1	5	14
GPTMS0.25-PEG200-N-TEOS60-S-c	4	3	1	3	5	16
GPTMS0.25-PEG200-N-TEOS60-S-d	5	3	1	1	5	15
GPTMS0.25-PEG200-N-TEOS60-S-e	4	3	1	1	5	14
GPTMS0.25-PEG200-N-TEOS60-S-f	5	3	1	2	5	16
TPI0.25-PEG200-N-TEOS60-S-a	3	5	1	4	4	17
TPI0.5-PEG200-N-TEOS60-S-a	1	4	1	1	1	8
TPI1.0-PEG200-N-TEOS30-S-a	5	5	2	4	5	21
TPI0.5-PEG200-N-TEOS30-S-a	5	5	2	4	5	22
TPI0.1-PEG200-N-TEOS30-S-a	5	5	1	3	5	19
TPI0.25-PEG200-N-TEOS30-S-a	4	5	1	4	5	19
TPI0.25-PEG2000-N-TEOS30-S-a	1	5	1	3	1	11
TPI0.25-PEG2000-N-TEOS30-S-b	1	5	1	5	2	14
TPI0.25-PEG2000-N-TEOS30-S-c	1	5	1	4	1	12
TPI0.25-PEG200-N-TEOS30-S-b	4	5	1	4	5	19
TPI1.0-PEG200-N-TEOS30-S-c	5	5	3	4	5	22
TPI1.0-PEG200-N-TEOS30-S-d	5	4	3	3	5	20
TPI1.0-PEG200-N-TEOS30-S-e	5	4	3	3	5	20
TPI2.0-PEG200-N-TEOS30-S-a	4	2	3	4	4	17
TPI1.0-PEG200-C-TEOS30-S-a	4	5	2	3	4	18
TPI2.0-PEG200-C-TEOS30-S-a	4	5	3	5	4	21
TPI0.5-PEG200-C-TEOS30-S-a	4	3	3	3	4	17
TPI0.25-PEG200-C-TEOS30-S-a	5	3	2	2	4	16
TPI3.0-PEG200-C-TEOS30-S-a	3	5	1	5	4	18
TPI1.0-PEG2000-C-TEOS30-S-a	1	5	1	5	1	13
TPI0.5-PEG400-C-TEOS30-S-a	5	4	4	3	4	20
TPI0.33-PEG600-C-TEOS30-S-a	5	4	5	4	4	22
TPI0.2-PEG1000-C-TEOS30-S-a	1	5	2	3	3	14

Synthesized Materials and Their Properties

F

Table F.1. Table of materials synthesized for the project and their properties.

Material	Properties
GPTMS0.25-PEG200-N-TEOS60-S-a	Coupling agent: GPTMS molar ratio 0.25, polymer: PEG-200, TEOS mixing time 60 minuets, age time: ca. 5 days, other container.
GPTMS0.25-PEG200-N-TEOS60-S-b	Coupling agent: GPTMS molar ratio 0.25, polymer: PEG-200, TEOS mixing time 60 minuets, age time: ca. 5 days.
GPTMS0.25-PEG200-N-TEOS60-S-c	Coupling agent: GPTMS molar ratio 0.25, polymer: PEG-200, TEOS mixing time 60 minuets, age time: ca. 5 days, thinner.
GPTMS0.25-PEG200-N-TEOS60-S-d	Coupling agent: GPTMS molar ratio 0.25, polymer: PEG-200, TEOS mixing time 60 minuets, age time: 3 days.
GPTMS0.25-PEG200-N-TEOS60-S-e	Coupling agent: GPTMS molar ratio 0.25, polymer: PEG-200, TEOS mixing time 60 minuets, age time: 5 days.
GPTMS0.25-PEG200-N-TEOS60-S-f	Coupling agent: GPTMS molar ratio 0.25, polymer: PEG-200, TEOS mixing time 60 minuets, age time: 7 days.
TPI0.25-PEG200-N-TEOS60-S-a	Coupling agent: TPI molar ratio 0.25, polymer: PEG-200, TEOS mixing time 60 minuets, age time: 3 days.
TPI0.5-PEG200-N-TEOS60-S-a	Coupling agent: TPI molar ratio 0.5, polymer: PEG-200, TEOS mixing time 60 minuets, age time: 3 days.
TPI1.0-PEG200-N-TEOS30-S-a	Coupling agent: TPI molar ratio 1.0, polymer: PEG-200, TEOS mixing time 30 minuets, age time: 3 days.
TPI0.5-PEG200-N-TEOS30-S-a	Coupling agent: TPI molar ratio 0.5, polymer: PEG-200, TEOS mixing time 30 minuets, age time: 3 days.
TPI0.1-PEG200-N-TEOS30-S-a	Coupling agent: TPI molar ratio 0.1, polymer: PEG-200, TEOS mixing time 30 minuets, age time: 3 days.
TPI0.25-PEG200-N-TEOS30-S-a	Coupling agent: TPI molar ratio 0.25, polymer: PEG-200, TEOS mixing time 30 minuets, age time: 3 days.
TPI0.25-PEG2000-N-TEOS30-S-a	Coupling agent: TPI molar ratio 0.25, polymer: PEG-2000, TEOS mixing time 30 minuets, age time: 3 days, at 55 °C, pre-melt of PEG-2000 and THF.
TPI0.25-PEG2000-N-TEOS30-S-b	Coupling agent: TPI molar ratio 0.25, polymer: PEG-2000, TEOS mixing time 30 minuets, age time: 3 days, at 55 °C, melting of PEG-2000.
TPI0.25-PEG2000-N-TEOS30-S-c	Coupling agent: TPI molar ratio 0.25, polymer: PEG-2000, TEOS mixing time 30 minuets, age time: 3 days, at 55 °C, melting of PEG-2000, addison of THF before TEOS and before aging
TPI0.25-PEG200-N-TEOS30-S-b	Coupling agent: TPI molar ratio 0.25, polymer: PEG-2000, TEOS mixing time 30 minuets, age time: 3 days, addision of boric acid: 0.1 molar ratio

Table F.2. Table of materials synthesized for the project and their properties, continued.

Material	Properties
TPI1.0-PEG200-N-TEOS30-S-c	Coupling agent: TPI molar ratio 1.0, polymer: PEG-200, TEOS mixing time 30 minuets, age time: 3 days, thinnest.
TPI1.0-PEG200-N-TEOS30-S-d	Coupling agent: TPI molar ratio 1.0, polymer: PEG-200, TEOS mixing time 30 minuets, age time: 3 days, thin.
TPI1.0-PEG200-N-TEOS30-S-e	Coupling agent: TPI molar ratio 1.0, polymer: PEG-200, TEOS mixing time 30 minuets, age time: 3 days, thinner.
TPI2.0-PEG200-N-TEOS30-S-a	Coupling agent: TPI molar ratio 2.0, polymer: PEG-200, TEOS mixing time 30 minuets, age time: 3 days.
TPI1.0-PEG200-C-TEOS30-S-a	Coupling agent: TPI molar ratio 1.0, polymer: PEG-200, TEOS mixing time 30 minuets, age time: 3 days, catalyzed by DBTL.
TPI2.0-PEG200-C-TEOS30-S-a	Coupling agent: TPI molar ratio 2.0, polymer: PEG-200, TEOS mixing time 30 minuets, age time: 3 days, catalyzed by DBTL.
TPI0.5-PEG200-C-TEOS30-S-a	Coupling agent: TPI molar ratio 0.5, polymer: PEG-200, TEOS mixing time 30 minuets, age time: 3 days, catalyzed by DBTL.
TPI0.25-PEG200-C-TEOS30-S-a	Coupling agent: TPI molar ratio 0.25, polymer: PEG-200, TEOS mixing time 30 minuets, age time: 3 days, catalyzed by DBTL.
TPI3.0-PEG200-C-TEOS30-S-a	Coupling agent: TPI molar ratio 3.0, polymer: PEG-200, TEOS mixing time 30 minuets, age time: 3 days, catalyzed by DBTL.
TPI1.0-PEG2000-C-TEOS30-S-a	Coupling agent: TPI molar ratio 1.0, polymer: PEG-2000, TEOS mixing time 30 minuets, age time: 3 days, at 55 °C, melting of PEG-2000, catalyzed by DBTL.
TPI0.5-PEG400-C-TEOS30-S-a	Coupling agent: TPI molar ratio 0.5, polymer: PEG-400 molar ratio 0.5, TEOS mixing time 30 minuets, age time: 3 days, catalyzed by DBTL.
TPI0.33-PEG600-C-TEOS30-S-a	Coupling agent: TPI molar ratio 0.33, polymer: PEG-600 molar ratio 0.33, TEOS mixing time 30 minuets, age time: 3 days, catalyzed by DBTL.
TPI0.2-PEG1000-C-TEOS30-S-a	Coupling agent: TPI molar ratio 0.2, polymer: PEG-1000 molar ratio, TEOS mixing time 30 minuets, age time: 3 days, at 35 °C, melting of PEG-1000, catalyzed by DBTL.